

การออกฤทธิ์ของบาราคอลต่อการตายแบบอะพอพโทสิสภายในเซลล์พีลิบแก้ว



นางสาวสุพิมพ์ วงษ์ทองแท้

สถาบันวิทยบริการ

จุฬาลงกรณ์มหาวิทยาลัย

วิทยานิพนธ์นี้เป็นส่วนหนึ่งของการศึกษาตามหลักสูตรปริญญาวิทยาศาสตรมหาบัณฑิต

สาขาวิชาชีวเวชเคมี ภาควิชาชีวเคมี


คณะเภสัชศาสตร์ จุฬาลงกรณ์มหาวิทยาลัย

ปีการศึกษา 2549

ISBN 974-14-2032-3

ลิขสิทธิ์ของจุฬาลงกรณ์มหาวิทยาลัย

CELLULAR EFFECTS OF BARAKOL-INDUCED APOPTOSIS IN P19 CELLS



Miss Supim Wongtongtair

สถาบันวิทยบริการ
จุฬาลงกรณ์มหาวิทยาลัย

A Thesis Submitted in Partial Fulfillment of the Requirements
for the Degree of Master of Science in Biomedical Chemistry

Department of Biochemistry

Faculty of Pharmaceutical Sciences

Chulalongkorn University

Academic year 2006

ISBN 974-14-2032-3

Thesis Title CELLULAR EFFECTS OF BARAKOL-INDUCED APOPTOSIS IN
P19 CELLS
By Miss Supim Wongtongtair
Field of study Biomedical Chemistry
Thesis Advisor Associate Professor Duangdeun Meksuriyen, Ph.D.
Thesis Co-advisor Associate Professor Vimolmas Lipipun, Ph.D.

Accepted by the Faculty of Pharmaceutical Sciences, Chulalongkorn
University in Partial Fulfillment of the Requirements for the Master's Degree

..... Pornpen Pramyothin Dean of the Faculty of Pharmaceutical Sciences
(Associate Professor Pornpen Pramyothin, Ph.D.)

THESIS COMMITTEE

..... Niyada Kiatying-Angsulee Chairman
(Assistant Professor Niyada Kiatying-Angsulee, Ph.D.)

..... D. Meksuriyen Thesis Advisor
(Associate Professor Duangdeun Meksuriyen, Ph.D.)

..... Vimolmas Lipipun Thesis Co-advisor
(Associate Professor Vimolmas Lipipun, Ph.D.)

..... Pornthep Tiensiwakul Member
(Professor Pornthep Tiensiwakul, Ph.D.)

..... Chaiyo Chaichantipyuth Member
(Associate Professor Chaiyo Chaichantipyuth, Ph.D.)

สุพิมพ์ วงษ์ทองแท้ : การออกฤทธิ์ของบาราคอลต่อการตายแบบอะพอพโทซิสภายในเซลล์พืชบก
CELLULAR EFFECTS OF BARAKOL-INDUCED APOPTOSIS IN P19 CELLS อ. ที่ปรึกษา :
รศ.ดร. ดวงเดือน เมฆสุริยพันธ์, อ. ที่ปรึกษาร่วม : รศ.ดร. วิมลมาศ ลิปิพันธ์, 66 หน้า. ISBN
974-14-2032-3.

บาราคอลเป็นสารออกฤทธิ์สกัดได้จากใบขี้เหล็ก (*Cassia siamea* Lam.) ซึ่งเป็นสมุนไพรพื้นบ้านของไทยมีสรรพคุณเป็นยารักษาอาการนอนไม่หลับ ต่อมาจามีรายงานความเป็นพิษ เป็นผลให้มีการระงับใช้ยาซึ่งผลิตมาจากใบขี้เหล็ก อย่างไรก็ตามยังไม่มีรายงานเกี่ยวกับกลไกความเป็นพิษของบาราคอลในระดับเซลล์ ดังนั้นวัตถุประสงค์ของงานวิจัยนี้เพื่อศึกษากลไกความเป็นพิษระดับชีววิทยาโมเลกุลของบาราคอลต่อการตายแบบอะพอพโทซิสในเซลล์พืชบก โดยได้สกัดบาราคอลจากใบขี้เหล็กได้มวลร้อยละ 0.1 ของน้ำหนักใบขี้เหล็ก นำมาศึกษาความคงตัวของบาราคอลในสภาวะเลี้ยงเซลล์พบว่าบาราคอลยังคงตัวภายในเวลาที่จะทดสอบความเป็นพิษของบาราคอล จากผลการศึกษาพิษของบาราคอลต่อเซลล์ด้วยวิธี XTT พบว่าบาราคอลเป็นพิษต่อเซลล์เพิ่มขึ้นเป็นสัดส่วนโดยตรงกับความเข้มข้น โดยมีค่า IC_{50} เท่ากับ 1.5 มิลลิโมลลาร์ จึงนำมาศึกษารูปแบบการตายของเซลล์ด้วยวิธีต่างๆ ดังนี้ การวิเคราะห์ด้วยสี Hoechst 33342 พบว่าเซลล์ตายแบบอะพอพโทซิสเพิ่มขึ้นอย่างมีนัยสำคัญภายหลังได้รับบาราคอลเป็นเวลา 24 ชั่วโมง และเมื่อเติมสารต้านอนุมูลอิสระ N-acetyl-L-cysteine (NAC) หรือ glutathione (GSH) ก่อนใส่บาราคอล พบว่าเซลล์ตายแบบอะพอพโทซิสลดลงอย่างมีนัยสำคัญ ขณะที่การย้อมเซลล์ด้วยสี propidium iodide และวัดผลด้วยวิธีโฟลไซโตเมทรีพบว่าทำให้วัฏจักรเซลล์ระยะ G_0/G_1 เปลี่ยนแปลงไปจากกลุ่มควบคุม จากนั้นวัดปริมาณอนุมูลอิสระภายในเซลล์ที่ได้รับบาราคอลโดยใช้สี 2',7'-dichlorodihydrofluorescein diacetate (DCFH-DA) และวิเคราะห์ด้วยวิธีโฟลไซโตเมทรี พบว่าปริมาณอนุมูลอิสระเพิ่มขึ้นอย่างมีนัยสำคัญภายในเวลา 2 ชั่วโมง และเมื่อให้เซลล์ได้รับสารต้านอนุมูลอิสระ NAC หรือ GSH ก่อนได้รับบาราคอลพบว่าเซลล์สามารถเพิ่มอัตราการอยู่รอดได้ใกล้เคียงกับกลุ่มควบคุม จากนั้นวิเคราะห์ชนิดของอนุมูลอิสระที่มีบทบาทสำคัญในการเกิดพิษต่อเซลล์ที่ได้รับบาราคอล โดยใช้เอนไซม์และตัวยับยั้งเอนไซม์ที่อยู่ในกระบวนการกำจัดอนุมูลอิสระคือ manganese(III)tetrakis (4-benzoic acid) porphyrin chloride (MnTBAP), catalase และ sodium formate พบว่าอนุมูลอิสระชนิด hydroxyl มีบทบาทสำคัญทำให้เซลล์ที่ได้รับบาราคอลตายแบบอะพอพโทซิส จากนั้นวัดการทำงานของเอนไซม์ caspase-9 ในเซลล์ที่ได้รับบาราคอลพบว่าเพิ่มขึ้นอย่างมีนัยสำคัญเมื่อเทียบกับกลุ่มควบคุม โดยสรุปบาราคอลมีผลไปเพิ่มอนุมูลอิสระและไปเหนี่ยวนำให้เอนไซม์ caspase-9 ทำงานเพิ่มขึ้น ทำให้เซลล์พืชบกตายแบบอะพอพโทซิสในที่สุด

ภาควิชา.....ชีวเคมี.....ลายมือชื่อนิสิต.....สุพิมพ์.....วงษ์ทองแท้.....
สาขาวิชา.....ชีวเวชเคมี.....ลายมือชื่ออาจารย์ที่ปรึกษา.....ดร. ดร.....
ปีการศึกษา.....2549.....ลายมือชื่ออาจารย์ที่ปรึกษาร่วม.....ดร.ดร.....

4676618133 : MAJOR BIOMEDICINAL CHEMISTRY

KEY WORD: Barakol / P19 cells / Apoptosis / Reactive oxygen species / Caspase-9

SUPIM WONGTONGTAIR : CELLULAR EFFECTS OF BARAKOL-INDUCED APOPTOSIS IN P19 CELLS. THESIS ADVISOR : ASSOC. PROF. DUANGDEUN MEKSURIYEN, Ph.D. THESIS COADVISOR : ASSOC. PROF. VIMOLMAS LIPIUN, Ph.D. 66 pp. ISBN 974-14-2032-3.

Barakol is an active constituent extracted from *Cassia siamea* Lam., which has been used in folk medicine for the treatment of insomnia, however, its toxicity was reported and became an important limitation of using this herbal drug. Since, the mechanism by which barakol-induced toxicity has not been elucidated, this study thus investigated the cytotoxicity of barakol and its underlying mechanism in P19 embryonic stem cells. The extraction of barakol was obtained with a 0.1% yield. The barakol stability in culture medium was clarified and its stability was still stable until 24 h. Treatment with barakol decreased cell viability in a time-dependent and a concentration-dependent manner measured by XTT assay with the IC_{50} value of 1.5 mM. Thus the type of cell death was evaluated. Hoechst 33342 assay showed a significant increase in apoptosis after 24 h incubation of barakol. While the pretreatment with antioxidants such as N-acetyl-L-cysteine (NAC) or glutathione (GSH) showed the significant decrease in apoptotic cells, suggesting that reactive oxygen species (ROS) may play a role in barakol-mediated apoptosis. Whereas the flow cytometric analysis using propidium iodide staining showed that the distribution G_0/G_1 cell cycle phase was different from control. The molecular mechanism of barakol-induced apoptosis via the generation of ROS was further elucidated. Treatment with barakol showed a significant increase in the ROS level, peaking at 2 h, detected by flow cytometry using 2',7'-dichlorodihydrofluorescein diacetate (DCFH-DA). Pretreatment of cells with NAC or GSH significantly inhibited ROS generation as well as apoptosis induced by barakol. To characterize ROS, the scavenging effects using manganese(III)tetrakis (4-benzoic acid) porphyrin chloride (MnTBAP, a superoxide dismutase mimetic), catalase (a hydrogen peroxide scavenger), and sodium formate (a hydroxyl radical scavenger) were performed. Pretreatment with MnTBAP or catalase had no significant change in ROS signal comparing to the barakol treated control, indicating the absence of the involvement of superoxide anion or hydrogen peroxide in this system. Pretreatment with sodium formate completely abolished the effect of barakol-induced ROS generation. The result indicated that the predominant ROS in barakol-induced apoptosis was hydroxyl radical. Furthermore, the activity of caspase-9 significantly increased after treatment of the cells with barakol. Taken together, induction of apoptosis in P19 cells by barakol was mainly associated with the ROS generation, mitochondrial dysfunction, and caspase-9 activation.

Department.....Biochemistry.....Student's signature.....Supim Wongtongtair
 Field of study....Biomedical Chemistry...Advisor's signature.....D. Luksuriyen
 Academic year..2006.....Co-advisor's signature.....Vimolmas Lipun

ACKNOWLEDGEMENTS

My sincere thanks to my advisor, Associate Professor Duangdeun Meksuriyen, my co-advisor Associate Professor Vimolmas Lipipun, from the very first day of my study in Biomedical Chemistry program have given me the advices, supervision, encouragement throughout this study.

I would like to express my appreciated to Associate Professor Chaiyo Chaichantipyuth, for giving advice in providing barakol. His excellent advice, guidance, encouragement, understanding and prompt action which have made the barakol extraction a reality.

I would like to special thank to Professor Pornthep Tiensiwakul of the Department of Clinical Microscopy, Faculty of Allied Health Science, Chulalongkorn University for his invaluable advisory in flow cytometry techniques.

I would like to thank to staffs and graduate students of the Department of Biochemistry, Faculty of Pharmaceutical Sciences, Chulalongkorn University, for their friendship and help during my work.

I am very much obliged and honored to the members of the Thesis Committee for their supportive attitude, constructive criticisms and for their invaluable discussions over my thesis.

This work was financially supported by Grants-in-Aid for Scientific Research DBG4780010 from the Thailand Research Fund (TRF) and from the Graduate School, Chulalongkorn University.

It would not be completed without expressing my heartfelt gratitude to my parents for their love, understanding, moral support and tremendous encouragements throughout my life.

CONTENTS

	Page
ABSTRACT IN THAI.....	iv
ABSTRACT IN ENGLISH.....	v
ACKNOWLEDGEMENTS.....	vi
CONTENTS.....	vii
LIST OF TABLES.....	viii
LIST OF FIGURES.....	x
LIST OF ABBREVIATIONS.....	xii
CHAPTER	
I INTRODUCTION.....	1
II LITERATURE REVIEW.....	5
III MATERIALS AND METHODS.....	12
IV RESULTS.....	18
V DISCUSSION AND CONCLUSION.....	41
REFERENCES.....	47
APPENDICES.....	56
VITA.....	66

สถาบันวิทยบริการ
จุฬาลงกรณ์มหาวิทยาลัย

LIST OF TABLES

Table	Page
1. The peak area of barakol for standard curve analyzed by HPLC.....	59
2. The percentage of recovery of barakol in culture condition at various time points analyzed by HPLC	59
3. The percentage of cytotoxicity of barakol-treated P19 cells in a concentration-dependent manner for 24 h.....	60
4. The percentage of cytotoxicity of barakol at the concentration of its IC ₅₀ (1.5 mM) – treated P19 cells at various time points (time dependency)	61
5. The percentage of apoptotic cells, detected by Hoechst 33342 assay induced by barakol in a concentration-dependent manner for 24 h.....	61
6. The percentage of of sub G ₀ /G ₁ and G ₀ /G ₁ phase by flow cytometry using propidium iodide, induced by barakol in a concentration-dependent manner for 24 h.....	62
7. The apoptotic percentage of barakol which pretreated P19 cells with 1 mM GSH or 1 mM NAC before the addition of barakol at its IC ₅₀ (1.5 mM) for 24 h.....	62
8. The fluorescence intensity in P19 cells quantitated by a flow cytometry using DCFH-DA, in response to 0.4 mM barakol treatment at various time points (time dependency).....	63
9. The DCFH-DA fluorescence intensity in P19 cells quantitated by a flow cytometry, in response to barakol treatment (0.4 mM) pretreatment with 1 mM NAC or 1 mM GSH prior to the addition of barakol and detected at 2 h after barakol treatment.....	63
10. The fluorescence intensity in P19 cells quantitated by a flow cytometry using DCFH-DA, pretreatment with 0.1 mM MnTBAP before the addition of 0.4 mM barakol for 2 h.....	64
11. The fluorescence intensity in P19 cells quantitated by a flow cytometry using DCFH-DA, pretreatment with 30,000 unit/ml catalase before the addition of 0.4 mM barakol for 2 h.....	64

12. The fluorescence intensity in P19 cells quantitated by a flow cytometry using DCFH-DA, pretreatment with 1 mM sodium formate before the addition of 0.4 mM barakol for 2 h.....65
13. Fluorometric assay of caspase-9 activity in P19 cells using caspase-9 fluorometric assay kit LEHD-AFC in response to barakol treatment.....65



สถาบันวิทยบริการ
จุฬาลงกรณ์มหาวิทยาลัย

LIST OF FIGURES

Figure	Page
1. Proposed diagram of experimental design to elucidate the molecular mechanism of barakol-induced apoptosis.....	4
2. The conversion reaction of barakol, anhydrobarakol and anhydrobarakol hydrochloride	20
3. HPLC chromatograms of barakol in culture conditions.....	21
4. The stability study of barakol in culture conditions	22
5. The overlaid spectrum scanned at UV wavelength	23
6. Barakol-induced cytotoxicity in P19 cells	24
7. Morphological analysis of nuclear chromatin in P19 cells stained with Hoechst 33342 using fluorescence microscope	26
8. Data analysis of nuclear chromatin in P19 cells stained with Hoechst 33342 using fluorescence microscope	27
9. Flow cytometric analysis showing the effects of barakol-induced cell cycle variation and apoptosis in P19 cells	29
10. Hoechst 33342 staining analysis for the effects of antioxidants on barakol-treated P19 cells	30
11. Effect of antioxidants, NAC or GSH, on barakol-induced apoptosis in P19 cells	31
12. Time-dependent ROS formation in barakol-treated P19 cells.....	33
13. The effects of NAC and GSH on the generation of ROS induced by barakol were using specific fluorescence dye DCFH-DA and analyzed by flow cytometry.....	34
14. Effect of MnTBAP, a SOD mimetic, on barakol-treated cells analyzed by DCFH-DA staining	36
15. Effect of catalase, a hydrogen peroxide scavenger, on barakol-treated cells analyzed by DCFH-DA staining.....	37
16. Effect of sodium formate, a hydroxyl radical scavenger, on barakol-treated cells analyzed by DCFH-DA staining	38

17. Measurement of caspase-9 activity	40
18. Schematic illustrating possible effects of barakol on cellular redox and apoptosis	46



สถาบันวิทยบริการ
จุฬาลงกรณ์มหาวิทยาลัย

LIST OF ABBREVIATIONS

AFC	7-amino-4-trifluoromethyl coumarin
ANOVA	Analysis of variance
Apaf-1	apoptosis protease activating factor 1
ATCC	American Type Culture Collection
Bcl-2	B-cell leukemia/lymphoma 2
CAD	caspase-activated DNase
CARDs	caspase recruitment domains
CAD/DFF40	caspase-activated DNase/ DNA fragmentation factor
CO ₂	carbon dioxide
cyt <i>c</i>	cytochrome <i>c</i>
DCF	2',7'-dichlorofluorescein
DCFH	2',7'-dichlorodihydrofluorescein
DCFH-DA	2',7'-dichlorodihydrofluorescein diacetate
°C	degree Celsius (centigrade)
DFF	DNA fragmentation factor
DMSO	dimethylsulfoxide
DNA	deoxyribonucleic acid
DNase	deoxyribonuclease
et al.	et alii, and others
FADD	Fas-associated death domain
FasL	Fas ligand

FBS	fetal bovine serum
g	grams
GSH	glutathione
GSSG	glutathione disulfide
h	hour
HCl	hydrochloric acid
H ₂ O ₂	hydrogen peroxide
HOAc	glacial acetic acid
HPLC	high performance liquid chromatography
H ₂ SO ₄	sulfuric acid
IC ₅₀	median inhibitory concentration
LEHD-AFC	leucine-glutamic acid-histidine-aspartic acid-(7-amino-4-trifluoromethyl coumarin)
α-MEM	alpha-minimum essential medium
MEM	minimum essential medium
MeOH	methyl alcohol
mg	milligram (s)
μg	microgram (s)
μl	microlitre (s)
min	minute (s)
ml	mililitre (s)
mm	millimeter (s)

mM	millimolar
MnTBAP	manganese(III)tetrakis (4-benzoic acid) porphyrin chloride
NAC	N-acetyl-L-cysteine
NADPH	nicotinamide adenosine dinucleotide phosphate
Na ₂ CO ₃	sodium carbonate
NCS	newborn calf serum
NMR	nuclear magnetic resonance
O ₂ ^{•-}	superoxide anion
OD	optical density
OH [•]	hydroxyl radical
PBS	phosphate buffered saline
pH	the negative logarithm of hydrogen ion concentration
PI	propidium iodide
PMS	phenazine methosulfate
RNase	ribonuclease
ROS	reactive oxygen species
SEM	standard error of mean
SOD	superoxide dismutase
SPE	solid phase extraction
TNF- α	tumor necrotic factor-alpha
TNFR	tumor necrotic factor receptor
t _R	retention time

UV	untraviolet
V	volt
XTT	2, 3-bis[2-methoxy-4-nitro-5-sulphonyl]-2H-tetrazolium- 5-carboxanilide



สถาบันวิทยบริการ
จุฬาลงกรณ์มหาวิทยาลัย

CHAPTER I

INTRODUCTION

Insomnia is a sleep problem which could happen in every one such as elderly, child and pregnant woman (Kamel et al., 2006; Nunes and Cavalcante, 2005; Sahota et al., 2003). These symptoms are usually treated by insomnia drugs or anxiolytic drugs. The anxiolytic drugs are available such as diazepam or chlordiazepoxide. These drugs work by chemically altering a specific receptor present on neuronal cell membranes, a reaction that involves the neurotransmitter gamma-aminobutyric acid (GABA). These drugs act immediately and show a great efficacy in reducing anxiety. However, they may produce certain undesirable effects, such as sedation, impaired cognition, potentiation of other depressants, and development of tolerance, dependence, and addiction (Salzman, 1991). In addition, several studies reported about the effects of insomnia drug in the pregnant and the embryo development (Coyle et al., 1976; Ornoy et al., 1998). Not only in human but the effects from insomnia drug also make the teratogenic effects in animal as well (Ornoy et al., 1998; Nagele et al., 1983). The general anxiolytic drug such as diazepam or benzodiazepines was reported the effect on embryonic cell *in vitro* (Ornoy et al., 1998; Nagele et al., 1983).

Barakol is a biologically active constituent of *Cassia siamea* Lam, which has been traditionally used for the treatment of insomnia and various other medical conditions in Southeast Asia, including Thailand. Dopamine agonist-like effects and possible serotonergic properties are proposed to explain the anxiolytic effect of barakol (Thongsaard et al., 1996; Thongsaard et al., 1997). The effects of barakol on the elevated plus-maze were compared to determine whether barakol exhibited a similar behavioural profile to diazepam, an established anxiolytic drug. *C. siamea* tablet was commercially available in 1998 for the treatment of insomnia. These tablets could induce sleepiness in healthy subjects and also improved quality of sleep in insomniac volunteers (Pooviboonsuk et al., 2000). However, the hepatotoxicity of barakol was first reported (Hongsirinirachorn et al., 2003). Barakol showed hepatotoxicity in human hepatoma HepG2 cells (Lawanprasert et al., 2001). However, the mechanism of cytotoxicity induced by barakol is still unclear.

Teratocarcinoma cells including P19 mouse embryonal carcinoma cell line are pluripotent, exhibiting similar characteristics to undifferentiation embryonic and fetal cell types. P19 cells are a useful tool to investigate the mechanism of teratogenesis (Jones-Villeneuve et al., 1982; McBurney et al., 1982). Developmentally, pluripotent P19 cells give rise to the formation of cell derivatives of all three germ layers and appear to differentiate by the same mechanisms as normal embryonic stem cells (Bain et al., 1994; McBurney, 1993). P19 cells are induced to differentiate to neuroectodermal cells, including neurons, glia, and fibroblast-like cells by retinoic acid. Meanwhile, P19 cells also differentiate to mesodermal cells such as cardiac and skeletal muscle cells when they are first cultured as cell aggregates in the presence of dimethyl sulfoxide (DMSO) (Paquin et al., 2002). To understand the mechanism of barakol-induced cytotoxicity, P19 cells were selected to investigate the underlying mechanism induced by barakol.

Objective

To elucidate the molecular mechanism of barakol-induced apoptosis in P19 cells via the generation of reactive oxygen species and caspase activation.

Conceptual framework

Apoptosis, programmed cell death characterized by chromatin condensation and activation of caspases, can be initiated by two pathways including extrinsic pathway (death receptor-mediated) and intrinsic pathway (mitochondrial-mediated). The intrinsic pathway of apoptosis involves mitochondria. A variety of key events in apoptosis focused on mitochondria including changes in electron transport, altered mitochondrial oxidation–reduction, loss of mitochondrial membrane potential ($\Delta\psi_m$), and release of cytochrome *c* which followed by association with apoptosis protease activating factor 1 (Apaf-1), caspase-9, and ultimately caspase-3 cleavage (Shao et al., 1997; Wang, 2001). Increasing in ROS was often associated with intrinsic apoptosis (Adams, 2003; Kluza et al., 2005; Takahashi et al., 2003; Droge, 2002).

ROS, including free radical O_2^{\bullet} are dismutated by SOD via generation of H_2O_2 lead to the oxidation of glutathione to form glutathione disulfide (GSSG), thereby reducing the ratio of glutathione to glutathione disulfide (Takahashi et al., 2003). In a state of iron excess, free iron becomes available to catalyze the conversion of H_2O_2 to

highly toxic free radicals such as hydroxyl radical (OH^\bullet). Intracellular ROS levels may decrease through antioxidant such as N-acetyl-L-cysteine (NAC), a precursor for glutathione (GSH). Glutathione has been shown to scavenge free radicals. Due to the mitochondria dysfunction, ROS was released to cytosol. Previous studies have shown that the majority apoptosis in many cells is accompanied by upregulation of ROS, resulting in high ROS production leading to trigger apoptotic protein and ultimately apoptosis (Kluza et al., 2005; Kling et al., 2005; Adams, 2003; Lin et al., 2003; Pearl-Yafe et al., 2004; Junn et al., 2001). In this study, we investigated the molecular cytotoxicity of barakol in P19 embryonic stem cells via ROS generation which downstream affected caspase 9-activation.

Experimental design

To elucidate the molecular mechanism of barakol-induced apoptosis, P19 cells were used. The methods were designed as the followings (Figure 1). Cell viability was measured by XTT assay. Apoptotic cell death was detected by fluorescence microscopy staining with Hoechst 33342 and with propidium iodide (PI). Barakol-generated ROS was investigated by flow cytometry using 2', 7'-dichlorodihydro fluorescein diacetate (DCFH-DA). Moreover, the protective effect of antioxidant(s) on barakol-treated P19 cells was also implemented. The antioxidants NAC and GSH were used to confirm barakol-induced apoptosis via ROS generation. Moreover, ROS which play an important role in this mechanism was defined. Characterization of ROS was performed by using SOD mimetic (MnTBAP) for the measurement of O_2^\bullet generation, catalase to clarify H_2O_2 clearance, and sodium formate to clarify the OH^\bullet . Caspase-9 activation assay was performed and fold-increase in caspase-9 activity was determined by comparing the results with the level of un-induced control.

Contributions of the study

1. Understanding of the mechanism of cell death induced by barakol in P19 cells.
2. These studies lay the groundwork for further investigations into the mechanisms of barakol mediated birth defects in animal model.

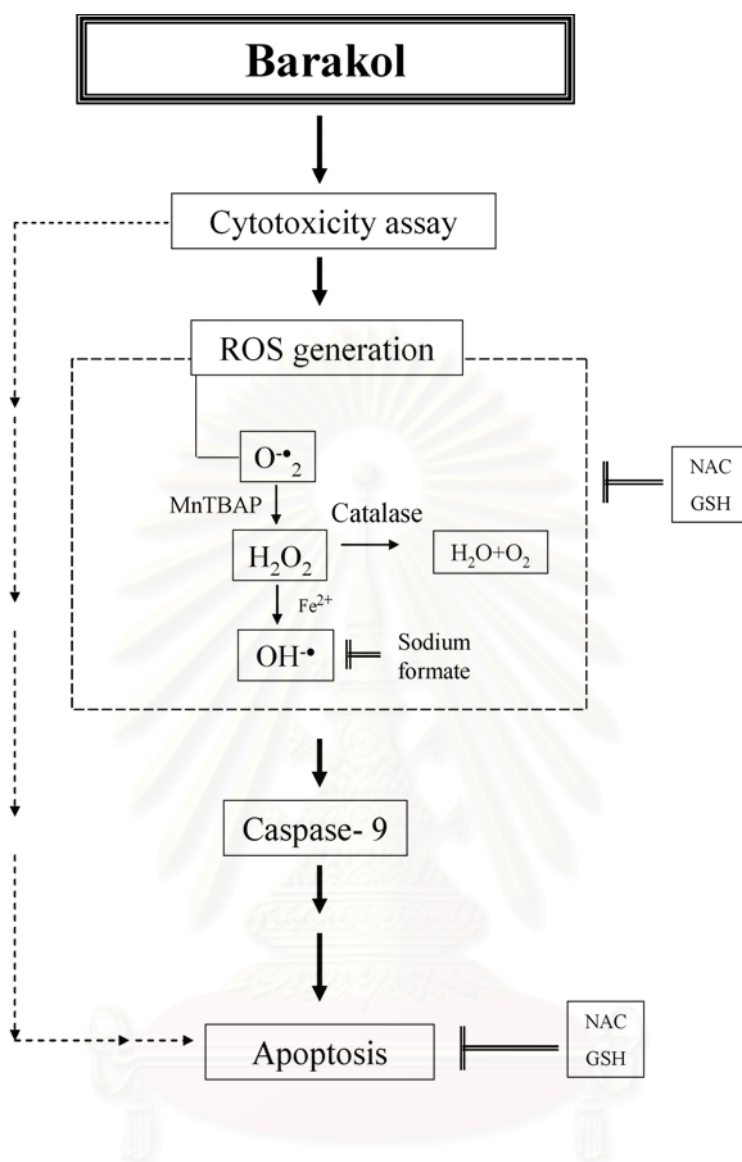


Figure 1 Proposed diagram of experimental design to elucidate the molecular mechanism of barakol-induced apoptosis.

สถาบันวิจัยชีววิทยา
จุฬาลงกรณ์มหาวิทยาลัย

CHAPTER II

LITERATURE REVIEW

Barakol

Cassia siamea Lam. has been consumed for centuries as an ingredient of a Thai curry. Young leaves and flowers of *C. siamea* were used as a folk medicine to treat insomnia, diabetes, hypertension, asthma, and constipation. Barakol, 3a,4-dihydro-3a,8-dihydroxy-2,5-dimethyl-1,4-dioxaphenalene is found to be an active constituent extracted from the leaves of *C. siamea*. Barakol is unstable and can be converted to anhydrobarakol by losing a molecule of water (Bycroft et al., 1970; Wagner et al., 1978). Barakol is very rapidly degraded by bases but with strong acids it forms anhydrobarakol hydrochloride which does not decompose at room temperature (Bycroft et al., 1970). In alkaline solution, barakol is degraded to cassiachromone (Bycroft et al., 1970; Wagner et al., 1978). In addition, the stability studies of barakol under various laboratory conditions using HPLC coupled with electrochemical detection demonstrated that barakol solutions can undergo auto-oxidation when exposed to the light or kept at high temperature. However, the stability studies demonstrated that barakol was suitable at 37 °C for in vitro and in vivo studies (Thongsaard et al., 2001).

In vitro studies have found that barakol inhibits K⁺-stimulated dopamine release from striatal slices of rat brain (Thongsaard et al., 1997). In addition, barakol could increase smooth muscle contraction in the isolated rat ileum under basal conditions and was found to inhibit norepinephrine suppressed smooth muscle contraction (Deachapunya et al., 2005). In animal studies, barakol has been shown to possess hypotensive activity (Suwan et al., 1992) and serotonergic receptor antagonist activity (Deachapunya et al., 2005), and it appears to function as an anxiolytic activity in exploratory behavioral testing (Thongsaard et al., 1996). Potential CNS activities of *C. siamea* were due to the presence of barakol, an anxiolytic agent extracted from the leaves of this plant (Arunlakshana., 1949; Hassanali et al., 1969; Thongsaard et al., 1996; Sukma et al., 2002). Thus the herbal product containing *C. siamea* was once approved to be commercially available in Thailand for the treatment of anxiety and insomnia

(Pooviboonsuk et al., 2000). After that, the herbal product containing *C. siamea* was reported about the hepatotoxicity in 2 patients of the 9 patients (Hongsinirachorn et al., 2003). Then the hepatotoxicity of barakol was demonstrated *in vitro* (Lawanprasert et al., 2001).

P 19 cells

P19 embryonic carcinoma cells, isolated from an experimental embryo-derived teratocarcinoma in mice, are pluripotent and can differentiate into cell types of all three germ layers, ectoderm, mesoderm, and endoderm, depending on their physical configurations (monolayer culture or cell aggregates) and their environment (Bain et al., 1994). These cells have the ability to change phenotype from malignant into non-malignant via the process of cellular differentiation. The exposure of P19 cell aggregates to retinoic acid leads to their differentiation into astrocytes and neurons (Jones-Villeneuve et al., 1983). Upon treatment with DMSO or hormone oxytocin, P19 cells differentiate into cardiac and skeletal muscle cells (Paquin et al., 2000). Several studies were reported about the differentiated mechanism or the important transcription factor involving in the differentiated processes (Schild et al., 2006; Jin et al., 2006; Pan et al., 2005; Jung et al., 2005).

P19 cells were a useful tool to investigate the toxic mechanisms induced by various substances such as nitrofen (Kling et al., 2004) or menadione (Chiou et al., 2000). Nitrofen appears to alter cell-redox (GSH: GSSG) by oxidative stress/ROS generation in the mitochondria. In addition, P19 cells were used as a model in several studies involving apoptotic mechanism. Allopregnanolone, a neurosteroid, is able to protect P19 neurons from apoptosis induced by N-methyl-D-aspartate (NMDA) (Xilouri and Papazafiri, 2006). When P19 tau cells were induced to undergo neural differentiation by treatment with retinoic acid, a remarkable increase in apoptosis was observed. In addition, the lifespan of the differentiated P19 tau cells was shorter than that of P19 wild-type cells (Tsukane and Yamauchi, 2006). The toxic effects of 6-hydroxy-dopamine also used P19 cells as a model (Woodgate et al., 1999). Therefore, P19 cells are a useful tool to investigate not only the toxicity mechanisms of the development of the embryonic

cells (Rajpert-De Meyts, 2006) but also for the study of mutagenesis as well (Sehlmeyer et al., 1996).

Patterns of cell death

Cells die in response to a variety of stimuli and during apoptosis they do so in a controlled, regulated fashion. This process of cell death requires time to take place after the initial insult (Kiechle et al., 2002). Apoptosis is a process in which cells play an active role in their own death which is why apoptosis is often referred to as cell suicide. Cells die through either of two distinct processes either necrosis or apoptosis. Apoptosis, or programmed cell death, is a normal component of the development and health of multicellular organisms. The apoptotic pattern is generally triggered by various stimuli including UV, light, and cellular stress (Shao et al., 1997; Saeki et al., 2002). Apoptotic pattern is defined by a series of cellular changes. Firstly the cell shrinks, loses contact with neighbouring cells or surrounding matrix and starts to display intracellular proteins on its surface. The chromatin in the nucleus condenses and the DNA is cleaved into small fragments of 180 base pairs, which lead to a characteristic of DNA laddering when subjected to gel electrophoresis. The plasma membrane then begins to show a bubbled appearance and small membrane bound bodies break off containing intracellular material which can include nuclear matter and cellular. The fragments are known as apoptotic bodies and they are quickly removed by phagocytes or by neighbouring cells. If this does not occur quickly enough, the plasma membrane and intracellular organelles can breakdown resulting in lysis of the fragments. This process is called secondary necrosis. This makes apoptosis distinct from another form of cell death called necrosis. Necrosis is an uncontrolled cell death that results from acute tissue injury and provokes an inflammatory response, characterised by cell swelling and mitochondrial damage leading to rapid depletion of energy levels, a breakdown of homeostatic control, cell membrane lysis and release of the intracellular contents, leading to an inflammatory response, with oedema and damage to the surrounding cells (Adams, 2003).

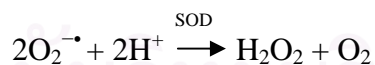
Apoptotic mechanism

Apoptotic cell death is an active process mediated by various signaling pathways, which include the caspase cascade and the stress-activated protein kinase pathways (Adams, 2003). There are at least two broad pathways that lead to apoptosis, an "extrinsic" and an "intrinsic" pathway. The extrinsic pathway begins outside a cell, when conditions in the extracellular environment determine that a cell must die. The extracellular signals such as anti-tumor agents, viral infections, and irradiation (Westendorp et al., 1995; Friesen et al., 1996; Muller et al., 1997; Rehemtulla et al., 1997) triggered death receptors that belong to the tumor necrotic factor receptor (TNFR) family. In particular, Fas (CD95/Apo-1), one of the most important receptor of TNFR family, plays a crucial role in maintaining the immune system by inducing apoptosis of immune cells as well as in killing harmful cells such as cancerous cells and bacterial or viral infected cells (Nagata, 1997). Binding of Fas ligand (FasL or CD95L) to the Fas receptor results in clustering of receptors and initiates the extrinsic pathway. Fas clustering recruits Fas-associated death domain (FADD) and pro-caspase-8 to the complex. Concentration of pro-caspase-8 results in its autocatalysis and its activation. The activated-caspase-8 cleaves pro-caspase-3, which then undergoes autocatalysis to form active caspase-3, a principle effector caspase of apoptosis.

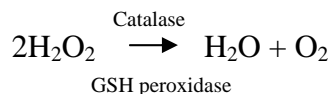
The intrinsic apoptotic pathway begins when an injury or the stress occur within the cell. In the intrinsic pathway, mitochondria play a central role in cell death by controlling cellular energy metabolism, production of ROS, and release of apoptotic factors into the cytosol. The most prominent pro-apoptotic factor released from mitochondria is cytochrome *c* (cyt *c*). Once released into the cytosol during apoptosis, cyt *c* binds to Apaf-1 thus forming a complex called the apoptosome, which recruits and activates pro-caspase-9 (Li et al., 1997; Liu et al., 1996). Thereafter, activated caspase-9 initiates the activation of downstream caspases, which cleave cellular substrates at specific tetra-peptide sequences on the carboxyl termini of aspartate residues. Disruption of an appropriate apoptotic response is implicated in the development of many disease states, including cancer, atherosclerosis and several degenerative diseases.

Reactive oxygen species leading to apoptosis

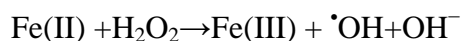
Cellular stress is caused by multiple factors including injury, inflammation, hypoxia, hormones, high concentrations of metabolites or xenobiotics, and excessive muscle work. “Metabolic stress” is created when the activity of a cell is stimulated, and could result in “oxidative stress” when ROS are produced intracellularly, particularly in mitochondria which participate in apoptosis. Furthermore, exogenous oxidants can generate “cytotoxic stress” that threatens survival of the cell (Kadenbach et al., 2004). At high concentrations, free radicals and radical-derived, nonradical reactive species are hazardous for living organisms and damage all major cellular constituents. At moderate concentrations, however, ROS play an important role as regulatory mediators in signaling processes (Droge et al., 2002). ROS are generated during normal processes of mitochondrial oxidative phosphorylation. Under physiological conditions, electrons carried by the electron transport chain can leak out of the pathway and pass directly to oxygen, generating $O_2^{\bullet-}$. Other sources of $O_2^{\bullet-}$ include enzymes such as cytochrome P450 in the endoplasmic reticulum, lipoxygenases, cyclooxygenases, xanthine oxidase and NADPH oxidase in the cytosol (Chen et al., 2003). The dismutation of $O_2^{\bullet-}$ by SOD results in the generation of H_2O_2 . The predominant forms are the copper-containing enzyme and the zinc-containing enzyme, located in the cytosol. The second type is the manganese containing SOD found in the mitochondrial matrix (Bandyopadhyay et al., 1999).



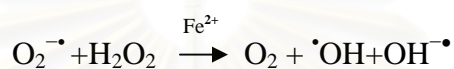
Under normal physiological conditions, hydrogen peroxide (H_2O_2) is converted into H_2O by glutathione peroxidase and catalase. GSH is not only present in mitochondria but also present in cytosol (Chen et al., 2003; Bandyopadhyay et al., 1999). In case of catalase, this enzyme is localized in the peroxisomes or the microperoxisomes (Bandyopadhyay et al., 1999).



However, this reaction is dependent upon the ratio of GSH : GSSG (oxidized form). If there is not enough reduced substrate ($2 \text{ GSH} \rightarrow \text{GSSG}$) available, H_2O_2 can react with Fe^{2+} to form hydroxyl radicals ($\cdot\text{OH}$), the highly toxic free radical, via the Fenton reaction. (Cadenas and Davies, 2000; Carmody and Cotter, 2001; Slater et al., 1995).



Additionally, the hydroxyl radical could also be generated through the metal catalyzed Haber-Weiss reaction as follows (Evens et al, 2004)



High concentration of ROS could induce apoptotic cell death in various cell types (Lee et al., 2005; Kling et al., 2005), suggesting that ROS contribute to cell death whenever they are generated in the cortex of the apoptotic process (Droge, 2002). ROS as an oxidant could passively attack cellular compound. Increases in ROS are often associated with apoptosis (Kluza et al., 2005; Kling et al., 2005; Takahashi et al., 2003). The generation of ROS disrupted mitochondrial membrane potential, decrease of Bcl-2 and increase of Bax leading to mitochondrial dysfunction. Release of apoptogenic factors from mitochondria, the best known of which is cyt *c*, leads to assembly of a large apoptosis-inducing complex called the apoptosome. Cysteine proteases (called caspases) are recruited to this complex and, following their activation by proteolytic cleavage, activate other caspases, which in turn target for specific cleavage a large number of cellular proteins.

Flow cytometry for the analysis of intracellular ROS

Flow cytometry is a technology that simultaneously measures and then analyzes multiple physical characteristics of single particles, usually cells, as they flow in a fluid stream through a beam of light. The measurements include a particle's relative size, relative granularity or internal complexity, and relative fluorescence intensity. These characteristics are determined using an optical-to-electronic coupling system that records

how the cell or particle scatters incident laser light and emits fluorescence (Becton Dickinson learning guide, 2002).

For ROS analysis, cells were stained with DCFH-DA, via a membrane bound esterase. In this way the dye is converted into DCFH and accumulated in the intracellular space of intact cells. The dye can interact with H_2O_2 or $\text{O}_2^{\bullet-}$ or OH^{\bullet} , forming DCF, whose fluorescence signal can be easily measured by flow cytometer. Thus, the total intracellular ROS level can be estimated.



The data can be presented as histogram plot or as a mean fluorescence signal characterizing the cell population under analysis (Boldyrev, 2000).

Flow cytometry for the analysis of the pattern of cell death

For DNA content analysis, special algorithms are used. The area under the curve is integrated; then the percentages of each population present are calculated. One of the major characteristics which have been used to assess apoptosis is the state and content of nuclear DNA. The latter is readily assessed by flow cytometric quantitation of red fluorescence from fixed propidium iodide-stained, RNase-treated cells. Propidium iodide fluorescence representation of apoptotic activity is heralded by sub G_0/G_1 events on DNA histograms (Nicoletti et al. 1991). Flow cytometry has been used to analyze numerous features of the apoptotic process (Lecoeur, 2002). Data were analyzed by bivariate analysis of \log_{10} forward-angle light scatter (FALS) or DNA signals (detected by propidium iodide fluorescence) of intact cells, in the region of high FALS or high SS and diploid [G_1] to tetraploid [G_2] DNA contents versus the DNA signals in the region of lower FALS or SS and/or sub G_0/G_1 DNA contents of the apoptotic cells. Thus, a more complete analysis of the apoptotic progression, and of the products of the so formed, may be revealed by two-parameter flow cytometric analysis than would be evident were DNA content the only feature monitored (Worrington et al., 2003).

CHAPTER III

MATERIALS AND METHODS

Materials

P19 cell line (CRL 1825) was obtained from American Type Culture Collection (Maryland, USA). Alpha minimum essential medium (alpha MEM) and newborn calf serum (NCS) were purchased from Gibco (California, USA). Fetal bovine serum (FBS) was obtained from Biochom AG (Berlin, Germany). Propidium iodide (PI), ribonuclease A, tetrazolium salt XTT (2, 3-bis [2-methoxy-4-nitro-5-sulfophenyl]-2H-tetrazolium-5-carboxanilide), Hoechst 33342, trypsin, sodium formate, catalase from bovine liver, deferoxamine mesylate, N-acetyl-L-cysteine (NAC), glutathione (GSH), phenazine methosulfate (PMS), propidium iodide (PI) and 2',7'-dichlorodihydrofluorescein diacetate were purchased from Sigma-Aldrich (St. Louis, MO, USA). Methanol was of HPLC grade and purchased from Labscan Inc. (Dublin, Ireland). Acetic acid, hydrochloric acid, sulfuric acid, and sodium carbonate were purchased from Merck (Darmstadt, Germany). Caspase-9 fluorometric assay kit was from Biovision Inc. (Mountain View, CA, USA). Manganese (III) tetrakis (4-benzoic acid) porphyrin chloride (MnTBAP) was from A.G. Scientific, Inc. (SanDiego, CA, USA). The solid phase extraction (SPE) column, Strata X model, was obtained from Phenomenex, (Torrance, CA, USA). All other chemicals were commercially available reagents or analytical reagent quality.

Methods

1. Extraction of barakol from *Cassia siamea*

Barakol was extracted from young leaves of *C. siamea*, which were obtained from a local Bangkok market. The leaves were cut into pieces and boiled twice with 0.5% sulfuric acid for 20 minutes. All fractions of water extract were filtrated, neutralized with sodium carbonate and extracted with dichloromethane. The dichloromethane fraction was concentrated under reduced pressure and the concentrated barakol extracted was shaken in cold water (ratio 1:1). The crude barakol was crystallized as greenish yellow needles which

were then washed and dissolved in methanol. Concentrated hydrochloric acid was finally added to obtain barakol hydrochloride, and the mixture was dried by vacuum filtration to form yellowish crystallized anhydrobarakol hydrochloride and purified by chromatography. When anhydrobarakol hydrochloride is dissolved in water, the reaction is reversed, and the product used in all the biological experiments is a barakol solution (Deachapunya et al., 2005).

2. Stability study of barakol

To clarify the enduring of barakol in culture condition, barakol in cell culture medium were analyzed. Barakol was added to the culture condition with cells and without cells, containing alpha MEM, 2.5 % FBS, 7.5% NCS, and incubated at 37 °C, 5% CO₂ for 0, 6, 18, 24 h. At the end of incubation time, each sample was applied to a solid phase extraction (SPE) with 0.45 micron filtration and analyzed by HPLC. For SPE condition, sample was applied to the SPE column, which was pre-washed with 1 ml of methanol and 2 ml of water, then applied 1 ml of sample. The column was then washed with 3 ml of 5% (v/v) methanol in water for four times. Finally, the column was eluted with 3 ml of methanol twice and the eluant was collected in a 1 ml auto-injector vial for HPLC analysis (Rouzer et al., 2002). The HPLC system consisted of a Shimadzu LC-10AD VP liquid chromatographic system equipped with SPD-M10A VP photodiode array detector (Shimadzu, Japan). Alltima HP C18 column (Deerfield, IL, USA) with 3- μ m particle size (150 x 4.6 mm i.d.) was used at ambient temperature (28 °C). The optimal system for detection was methanol and 1% acetic acid in water (20:80, v/v) as the mobile phase at a flow rate of 1 ml/min. The injection volume was 10 μ l, and the major wavelength was monitored at 249 nm.

3. Cell culture

P19 cells were grown in alpha-MEM supplemented with 2.5% FBS, 7.5% NCS in a humidified atmosphere of 5% CO₂ and 95% air at 37 °C. The cells were passaged for every 2–3 days.

4. Cell viability assay

4.1 Concentration-dependent study

P 19 cells were seeded at a density of 0.1×10^5 cells/ml in a 96-well plate. After 24 h, the cells were treated with barakol at various concentrations ranging from 0.05-4 mM for 24 h, and the cytotoxic 50% inhibitory concentration (IC_{50}) was determined. Cell viability was assessed by dye staining method using XTT at a final concentration of 1 mg/ml in the 96-well plate for 4 h at 37 °C. The XTT assay is based on the cleavage of yellow tetrazolium salt XTT to form an orange formazan dye by mitochondrial dehydrogenase in metabolic active cells, which are inactive shortly after cell death. The tetrazolium salts were mixed with PMS, the intermediate electron acceptor, for final concentration was 25 μ M. Therefore, this conversion only occurs in viable cells. The optical density (OD) was quantified at an absorbance of 450 nm using a reference wavelength of 620 nm (Lin et al., 2001). Cell viability was expressed as a percentage of the control culture. The percentage of cytotoxicity was calculated by the following equation:

$$\% \text{ cytotoxicity} = \frac{OD_{450 \text{ nm}} (\text{sample-blank}) \times 100}{OD_{450 \text{ nm}} (\text{control-blank})}$$

4.2 Time-course study

P 19 cells were seeded at a density of 0.1×10^5 cells/ml in a 96-well plate. After 24 h, the medium was discarded and replaced with medium containing 1.5 mM barakol (IC_{50}). Incubation with barakol was continued for 6-24 h. At the end of each time study, cell viability of P19 was assessed by tetrazolium salt XTT assay.

5. Measurement of apoptotic cells

Fluorescence microscopic assay using Hoechst 33342 and DNA flow cytometry method using PI were performed to investigate whether barakol could induce apoptosis.

5.1 Hoechst 33342 staining assay

Hoechst 33342, a fluorescence DNA and chromatin stain, was used for morphological studies. Hoechst 33342 experiments were performed in 96-well plates. After the incubation in serum supplemented medium for 24 h, P19 cells were exposed to barakol at various concentrations ranging from 0.2-1.5 mM for 24 h. They were stained with Hoechst 33342 at a final concentration of 10 µg/ml for 30 min in the dark at 37 °C. The morphological change in nuclear was visualized with a fluorescence microscope (model IX51, Olympus, Tokyo, Japan). The cells with brightly stained condensed chromatin, nuclear fragmentation or apoptotic bodies were considered as apoptotic cells.

5.2 Effect of antioxidants on barakol-induced apoptosis

P19 cells were pretreated with antioxidants, NAC or GSH, 1 mM for 30 min at 4°C for 30 min before adding barakol at the concentration of IC₅₀ value for 24 h. Treated cells were stained with Hoechst 33342 at a final concentration of 10 µg/ml for 30 min in the dark at 37 °C, visualized, and photographed under a fluorescence microscope. The amount of apoptotic cells were randomly counted as a percentage of the total population.

5.3 Flow cytometric analysis of apoptotic cells using propidium iodide staining

P19 cells were seeded in 6-well plates at a density of 2.5×10^5 cells/ml. The cells were further cultivated for 24 h and treated with barakol at 0.4 and 1.5 mM for 24 h. After barakol exposure, flow cytometric analysis was performed as described previously (Li et al., 2003). Briefly, treated cells were harvested and washed time with PBS, twice, then fixed in 2 ml cold 70% ethanol, and stored at 4 °C for 24 h. After washing with PBS, the cells were resuspended in PBS containing RNase A 100 µg/ml and incubated at 37 °C for 30 min. Propidium iodide was added to a final concentration of 40 µg/ml, and the mixture was then incubated at 37 °C for 30 min while protected from light (Glozak et al., 1996; Jérôme Kluza et al., 2005). Samples were analyzed for DNA content by a FACSort flow cytometer (Becton Dickinson, San Jose, CA, USA). Excitation was done at 488 nm, and emission filter at 600 nm. CellQuest™ Pro software (Becton Dickinson), was used for sub G₀/G₁ phase for DNA

distribution in apoptotic process. Ten thousand cells in each sample were analyzed and expressed as percentage of total cells.

6. Measurement of intracellular reactive oxygen species

6.1 Measurement of intracellular ROS formation

H₂O₂ production was monitored by flow cytometry using DCFH-DA. This dye is a stable nonpolar compound that readily diffuses into cells. Once inside the cells, the acetate groups of DCFH-DA are cleaved from the molecule by intracellular esterases to yield DCFH (McArdle, et al, 2005) which is trapped within the cells. Intracellular H₂O₂ or low-molecular weight peroxides, in the presence of peroxidases, oxidize DCFH to DCF, the highly fluorescence compound. Thus, fluorescence intensity is proportional to the amount of peroxides produced by the cells. The cells were rinsed and resuspended in ice-cold PBS (1×10⁶ cells/ml) and incubated with DCFH-DA at a final concentration of 5 μM for 30 min at 4° C. Then, cells were washed twice with ice cold PBS to remove the extracellular DCFH-DA and resuspended in PBS. Barakol was added in each sample at a concentration of 0.4 mM and incubated for various time intervals (30 min- 2 h) at 37 °C. The fluorescence intensity was measured by a FACScan flow cytometer (excitation at 488 nm; emission at 525 nm).

6.2 Effect of antioxidants on the generation of ROS in barakol-treated cells

To determine whether the antioxidants NAC and GSH effectively inhibited barakol-induced ROS generation, the cells were stained with DCFH-DA at a final concentration of 5 μM and pretreated with either NAC or GSH, at a concentration of 1 mM for 30 min at 4 °C before adding barakol at a final concentration of 0.4 mM for 2 h. The relative fluorescence intensity was analyzed by flow cytometry.

6.3 Characterization of ROS species

Cells were incubated with DCFH-DA at a concentration of 10 μM for 30 min at 4 °C, after which they were washed, collected, resuspended in PBS (1×10⁶cells/ml).

Pretreatment with 0.1 mM of MnTBAP (Sawyer et al., 2005), a permeable SOD which changed O_2^{\bullet} to hydrogen peroxide, or 30,000 unit/ml catalase (Zhang et al., 2001), enzyme which changed H_2O_2 to water and oxygen, or 1 mM sodium formate (Kuta et al., 2003), which could clear OH^{\bullet} from system, for 30 min at 4 °C. Then barakol at a concentration 0.4 mM was added and incubate at 37 °C for 2 h and analyzed fluorescence intensity by flow cytometer.

7. Measurement of caspase-9 activity

After treatment with barakol at the indicated concentrations, cells were washed with PBS and lysed in lysis solution. Activity of caspase-9 was detected by using Fluorometric Assay Kit according to the manufacturer's instructions (Biovision Mountain View, CA). In brief, cells were lysed in 50 μ l of cold lysis buffer, kept on ice for 10 min and centrifuged for 10 min at 3700 rpm, after which the supernatant was collected. Cell lysate was added to 50 μ l of reaction buffer and 5 μ l of fluorogenic substrates specific for caspase-9 (LEHD-AFC). After incubation at 37 °C for 2 h, the fluorescence intensity was detected by a fluorescence microplate reader with an excitation wavelength at 400 nm and an emission wavelength at 505 nm.

8. Statistical analysis

Data were expressed as mean \pm SEM. For differences between several mean values, analysis of variance (ANOVA) was performed. A Turkey multiple comparison test was used to determine which groups were significantly different from the control. Results were considered to have reached statistical significance when $P < 0.05$.

จุฬาลงกรณ์มหาวิทยาลัย

CHAPTER IV

RESULTS

1. Extraction of barakol from *C. siamea*

The re-crystallized barakol was obtained as greenish-yellow needles with a 0.1% yield. Concentrated hydrochloric acid was finally added to obtain anhydrobarakol HCl, and the mixture was dried by vacuum filtration to form yellowish crystallized anhydrobarakol HCl. The physical, greenish-yellow crystals, and spectroscopic characteristics of the barakol solution are very similar to that reported in previous studies (Chaichantipyuth, 1979). Barakol used in the present studies was anhydrobarakol HCl with a molecular weight of 251.4. When anhydrobarakol HCl is dissolved in water, the reaction is reversed, and the product used in all the biological experiments is a barakol solution (Figure 2). In this experiment, anhydrobarakol HCl was freshly prepared by dissolving in distilled water, wrapped with aluminum foil because barakol was unstable under light (Thongsaard et al., 2001).

2. Stability study of barakol

To elucidate the stability of barakol in culture medium under conditions similar to those that would be expected in cytotoxicity experiment, we determined the percentage of barakol recovery in culture medium containing alpha MEM plus 7.5% NCS and 2.5% FBS. Barakol was added to the cells culture condition and incubated at 37 °C, in humidified atmosphere of 5% CO₂ for 0, 6, 18, 24 h then each sample was filtered through the SPE column and analyzed by HPLC-DAD. Moreover, the stability of barakol in culture medium without cells was also clarified as a control.

Chromatogram of barakol showed a retention time of 7.7 ± 1.5 min (Figure 3A). After 24 h incubation, a little peak at a retention time of 39.9 ± 1.6 min was detected (Figure 3B). The quantity of barakol was determined from the appropriate peak area using the standard curve shown in Figure 4A. The percentage of barakol recovery in culture condition with cells significantly decreased after 24 h of incubation time (Figure 4B). While barakol in culture condition without cells, the barakol recovery started to

detected at 18 h significantly. The result showed that the cellular metabolism did not affect barakol stability in culture condition. Spectrophotometric analysis showed that barakol spectrum was different from the spectrum under the little peak at the retention time of 39.9 ± 1.6 min (Figure 5). The barakol spectrum demonstrated the maximum absorbance at 249 nm but the little peak of a degraded product was observed at 291 nm. However, the identification of the degraded product must be elucidated in further study. Since barakol was very slightly decrease at 24 h in culture medium condition then the study of barakol cytotoxicity could be investigated during 24 h incubation time. The cytotoxicity result could be assumed to be due to barakol.

3. Effect of barakol on the viability of P19 cells

To examine the barakol-induced cytotoxicity, cell viability was determined in P19 cells using XTT assay, the method which informed cell viability by detected enzyme mitochondria dehydrogenase in cytosol.

3.1. Concentration-dependent study

Since active dehydrogenase enzyme of living cells can cleave XTT to produce formazan, the amount of formazan is directly related to the number of living cells. After seeding in 96-well plate, P19 cells were cultivated in medium for 24 h resulting in the cell population in log phase. Then P19 cells treated with barakol with concentrations ranging from 0.05 to 2 mM and incubated at 37 °C for 24 h. The result showed that barakol reduced the viable cells in a concentration-dependent manner with an IC_{50} value of 1.5 mM (Figure 6A).

3.2. Time-course study

The exposure of P19 cells to 1.5 mM barakol, resulted in a time-dependent decrease of viable cells. Cell survival was gradually declined from 12 h ($87.60 \pm 0.59\%$) to 24 h ($49.19 \pm 0.49\%$) (Figure 6B). Time-dependent study showed reduction of enzyme dehydrogenase in mitochondria, therefore, it may imply that the function of mitochondria was significantly altered as early as 12 h after treatment.

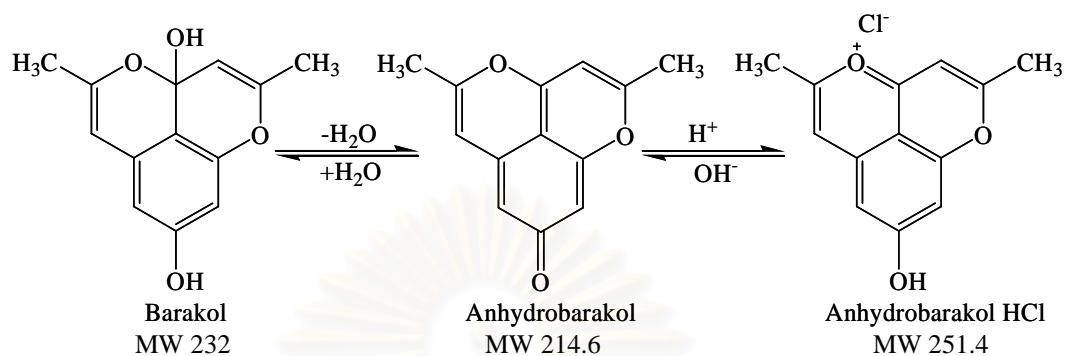
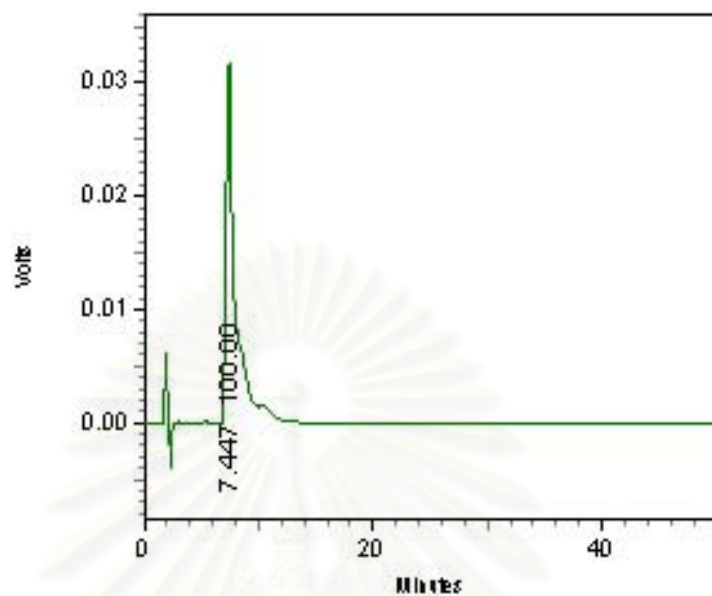


Figure 2 The conversion reaction of barakol, anhydrobarakol and anhydrobarakol hydrochloride.

สถาบันวิทยบริการ
จุฬาลงกรณ์มหาวิทยาลัย

(A)



(B)

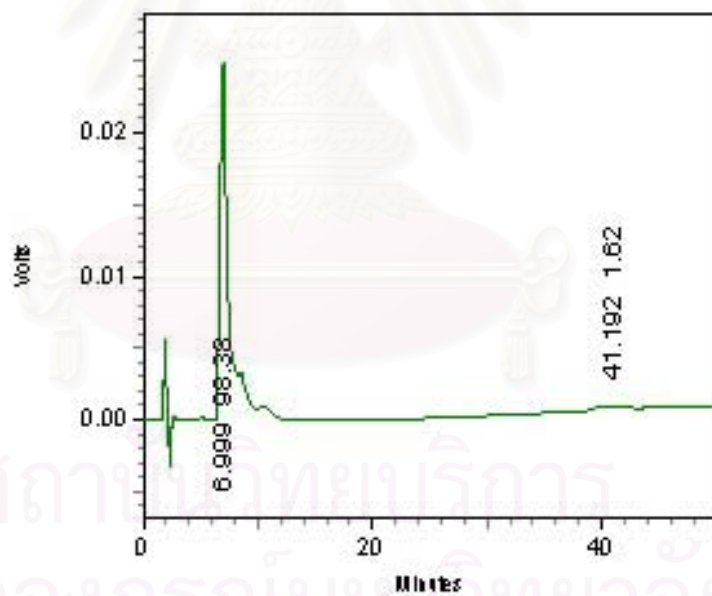
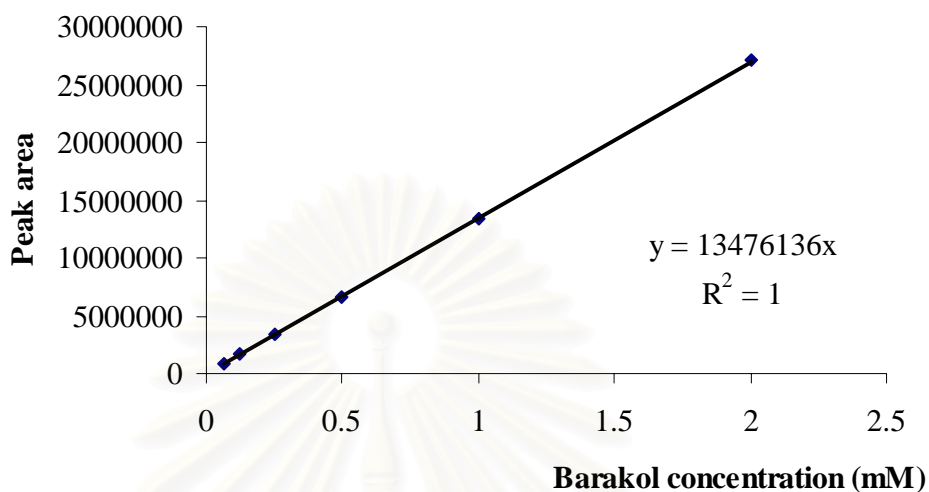
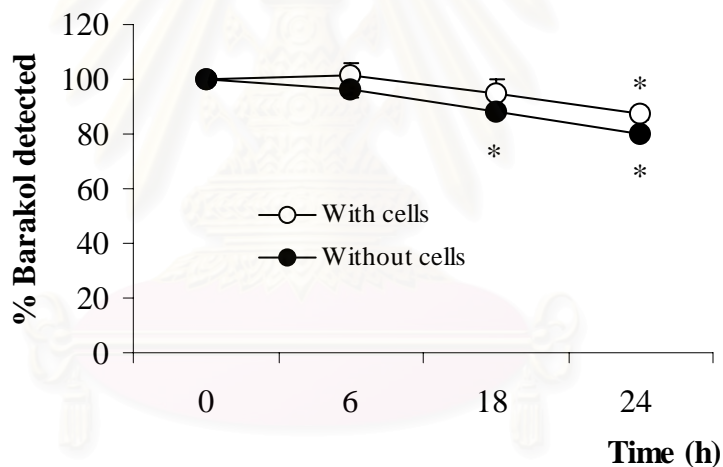


Figure 3 HPLC chromatograms of barakol in culture conditions, alpha MEM plus 7.5% NCS and 2.5% FBS with cells at various incubation times (A) 0 h (B) 24 h.

(A)



(B)

**Figure 4**

The stability study of barakol in culture conditions. (A) Standard curves for quantitation of barakol. Standards composed of water containing barakol at concentrations ranging from 0 to 2 mM were processed by HPLC analysis. (B) Barakol was incubated in culture condition, alpha MEM plus 7.5% NCS and 2.5% FBS, with cells and without cells, at various incubation times (0, 6, 18, 24 h). Each point represented the mean \pm SEM of three independent experiments, each performed in triplicate. * $P < 0.05$ compared to the culture medium at 0 h.

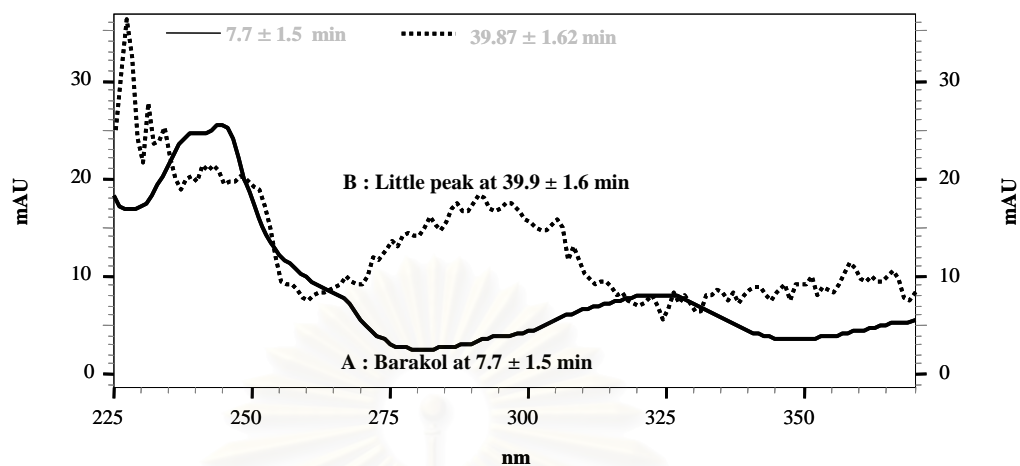


Figure 5 The overlaid spectrum scanned at UV wavelength. Barakol was incubated in culture condition for 24 h then barakol in culture medium was analyzed by HPLC. The chromatogram was scanned under UV wavelength, (A) barakol, (B) the degraded product at the retention time 39.9 ± 1.6 min.

สถาบันวิทยบริการ
จุฬาลงกรณ์มหาวิทยาลัย

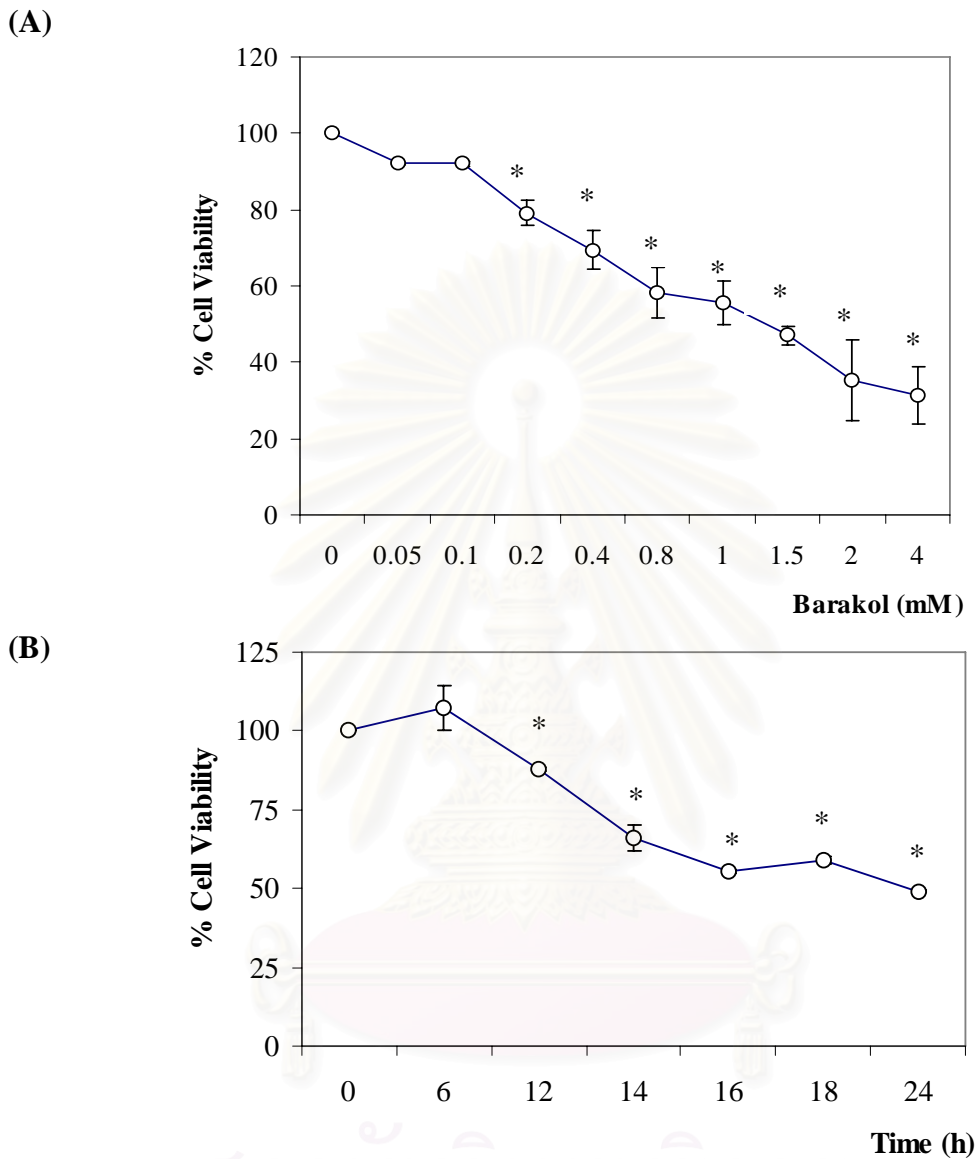


Figure 6 Barakol-induced cytotoxicity in P19 cells. (A) Concentration-dependency of barakol-induced cytotoxicity in the cells incubated with barakol at various concentrations ranging from 0-4 mM for 24 h. (B) Time dependency of barakol-induced cytotoxicity. All cells were exposed to medium with barakol at the IC_{50} value of 1.5 mM for 24 h. Data were expressed as % of viability measured by XTT assay. Each point represented the mean \pm SEM of three different experiments, each performed in triplicate. * $P < 0.05$ compared to the cells without barakol.

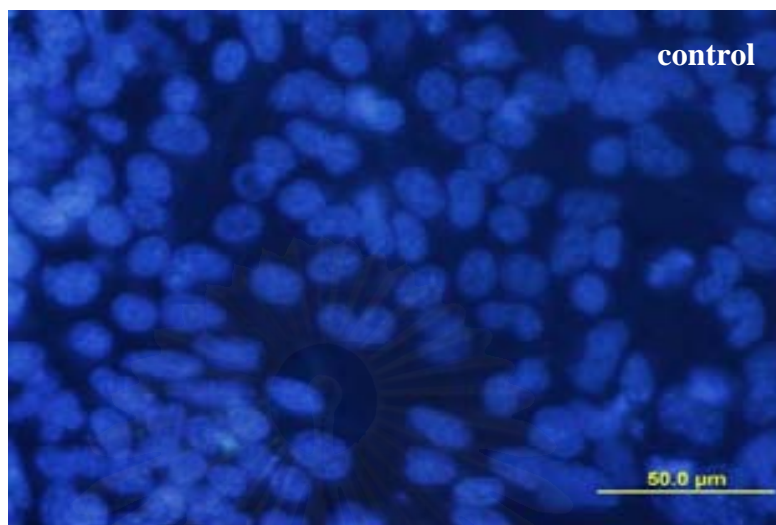
4. Barakol-induced apoptosis in P19 cells

To investigate whether the reduction in mitochondrial function might lead to apoptotic cell death, morphological observation of cell death using Hoechst 33342 staining and flow cytometric analysis staining with PI were performed.

4.1. Hoechst 33342 staining assay

Cytotoxicity mainly causes through either necrosis or apoptosis. This study was further characterized the death pattern by which barakol-induced cytotoxicity. Subconfluent (80%) P19 cells were treated with barakol at various concentrations ranging from 0.2-1.5 mM for 24 h. Nuclear staining with Hoechst 33342 demonstrated that control P19 cells had regular and round-shaped nuclei (Figure 7A). In contrast, the chromatin clumping in apoptotic nuclei, characteristic of early stage of apoptotic cells, were evidence in cells treated with barakol concentrations ranging from 0.2-1.5 mM (Figure 7B). Approximately $10.0 \pm 1.0\%$ of the treated cells showed apoptotic morphology after exposure with barakol at a concentration of 0.4 mM. Importantly, barakol at the IC_{50} value (1.5 mM) showed approximately $35.0 \pm 1.0\%$ apoptotic cells (Figure 8, Table 5), indicating that barakol-induced cytotoxicity mainly caused cell apoptosis. Since Hoechst 33342 staining has been used to determine the early stage and late stage of apoptosis (Piiper et al., 2002). However, barakol-treated cells for 24 h rarely showed the apoptotic body, sign of a late stage of apoptosis. Taken together with the XTT assay, these results indicated that barakol induced primarily apoptosis in a dose-dependent manner (Figure 8).

(A)



(B)

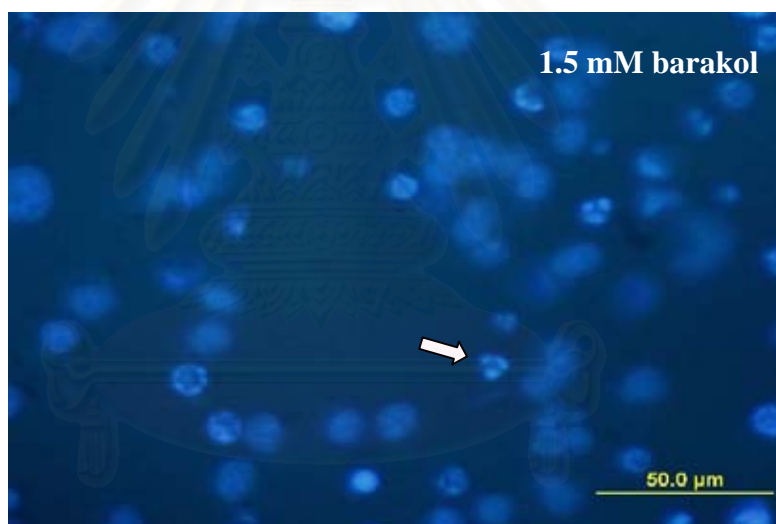


Figure 7 Morphological analysis of nuclear chromatin in P19 cells stained with Hoechst 33342 using fluorescence microscope. (A) In control, P19 cells were cultivated in medium for 24 h then 10 $\mu\text{g}/\text{ml}$ of Hoechst 33342 was stained, viable cells showed bright round nuclei with Hoechst 33342 staining. Apoptotic cells were hardly observed in control medium. (B) Barakol at a concentration 1.5 mM displayed chromatin condensation (arrow) and nuclear fragmentation. Scale bar = 50 μm .

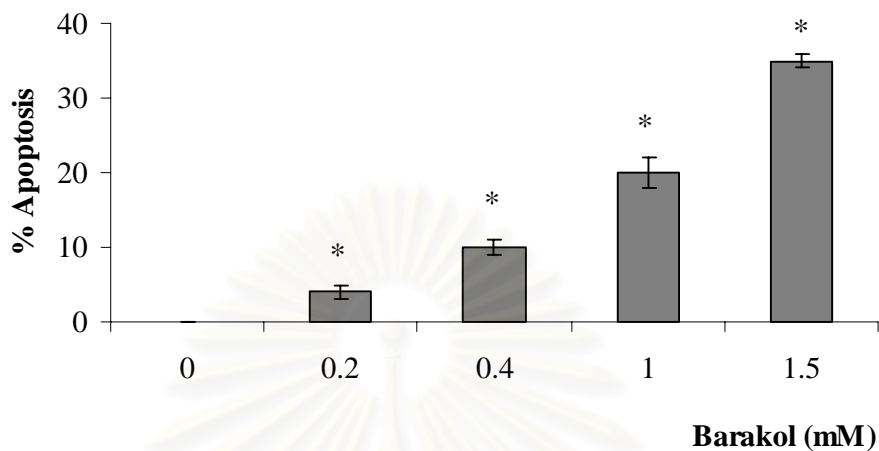


Figure 8 Data analysis of nuclear chromatin in P19 cells stained with Hoechst 33342 using fluorescence microscope. P19 cells incubated with barakol at concentrations ranging from 0.2-1.5 mM. After 24 h incubation, cells were stained with Hoechst 33342. The nuclear morphological change in nuclear was visualized with a fluorescence microscope. Data were expressed as the percentage of total cells. Each point represented the mean \pm SEM of three different experiments, each performed in triplicate. * P <0.05 compared to the cells without barakol.

4.2. Flow cytometric analysis of apoptotic cells using propidium iodide staining

The staining of PI, a well known dye for the detection of late apoptosis (Lecoeur, 2002) was used to clarify DNA content in P19 cells after exposure to barakol. The PI can stain DNA by intercalating between the base with a stoichiometry of one dye per 4-5 base pairs of DNA. The sub G₀/G₁ peak in flow cytometric detection is considered as an indicator of cell apoptosis as shown in Figure 9A. The results showed that the percentage of apoptotic cells (sub G₀/G₁ peak) increased from 2.3 ± 1.5% in control (Figure 9A) to 4.08 ± 1.2% in cells exposed to 0.4 mM barakol (Figure 9B) and to 6.01 ± 3% in cells exposed to 1.5 mM barakol (Figure 9C). The percentage of apoptotic cells (sub G₀/G₁ peak) slightly increased but not significantly (Figure 9D). However, barakol at the IC₅₀ concentration (1.5 mM) altered the distribution of cell cycle phase via G₀/G₁- phase and significantly decreased PI intensity value (Figure 9E).

4.3. Effect of antioxidants on barakol-induced apoptosis

ROS generation has been considered as a mechanism of various stimuli-induced apoptosis (Ohshima et al., 2004). To establish the correlation between barakol-induced apoptosis and ROS generation, the effect of antioxidants NAC and GSH in barakol-induced apoptosis was examined by using Hoechst 33342 staining assay. After pretreatment with 1 mM NAC or 1 mM GSH for 30 min, 1.5 mM barakol was added and incubated for 24 h. The control cells exhibited the bright round nuclei of living cells (Figure 10A) while barakol-treated cells exhibited DNA condensation (Figure 10B). The addition of antioxidant prior to barakol addition clearly protected P19 cells from apoptosis induced by barakol (Figures 10C and 10D). Importantly, barakol at the a concentration of 1.5 mM (IC₅₀) demonstrated 35.34 ± 1.15% apoptotic cells (Table 7). While the pretreatment with NAC or GSH decreased the apoptotic cells to 3.0 ± 1.0% and 3.34 ± 1.15%, respectively, which was nearly equal to the control (1.0 ± 1.0%) (Figure 11). This finding indicated the involvement of ROS in barakol-induced apoptosis.

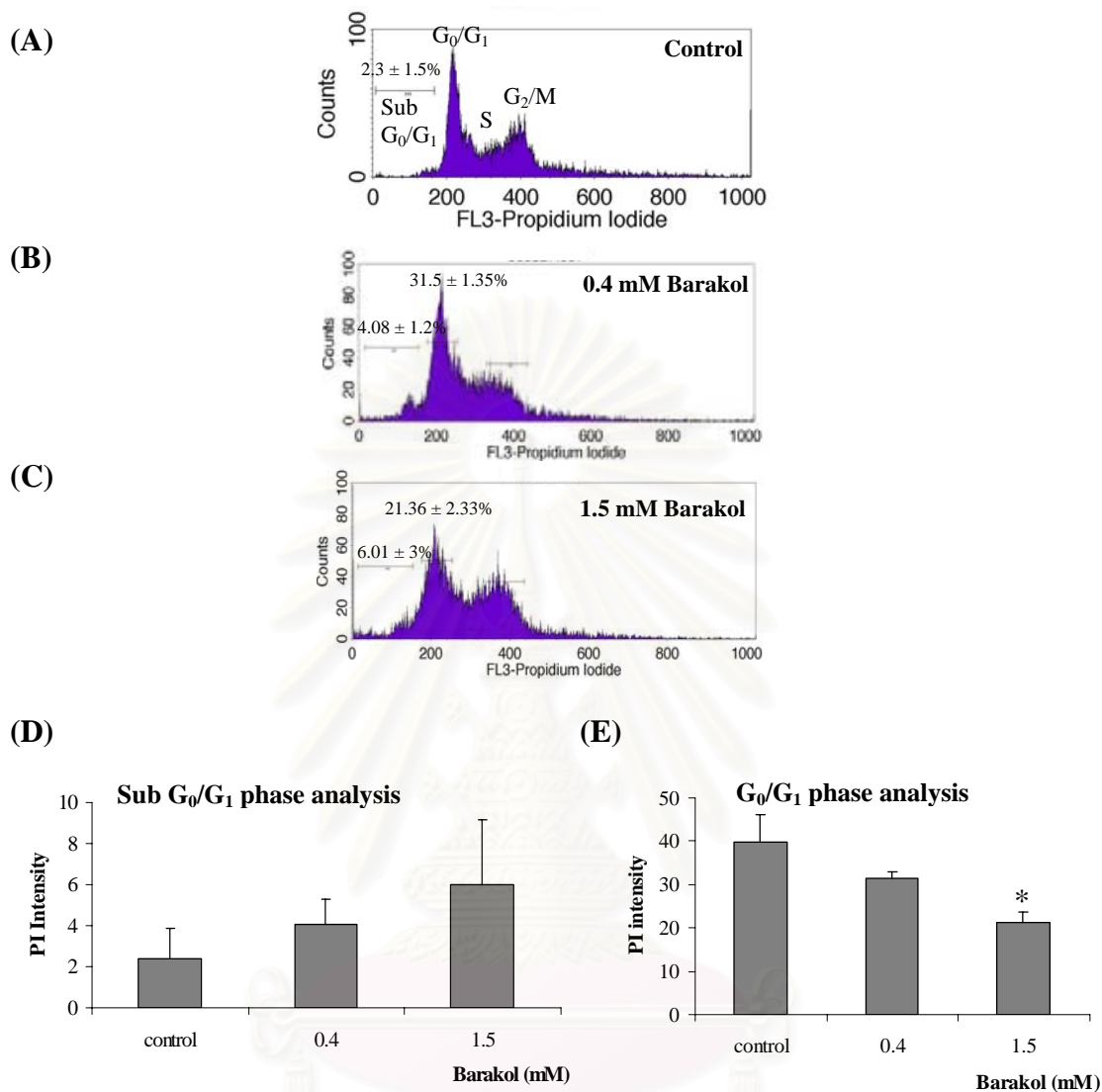


Figure 9 Flow cytometric analysis showing the effects of barakol-induced cell cycle variation and apoptosis in P19 cells. P19 cells were treated with barakol at concentrations of 0.4 and 1.5 mM for 24 h. Apoptotic cell death was accessed according to the percent of cells with sub G₀/G₁ peak as representative histogram of barakol-treated P19 cells compared with control (A), barakol at concentrations of 0.4 mM (B) and 1.5 mM (C). Determination of the duration of sub G₀/G₁ and G₀/G₁ phase in barakol-treated cells. Sub G₀/G₁ phase was determined (D) while G₀/G₁ phase was showed significantly decrease (E). Each point represented the mean ± SEM of three independent experiments.

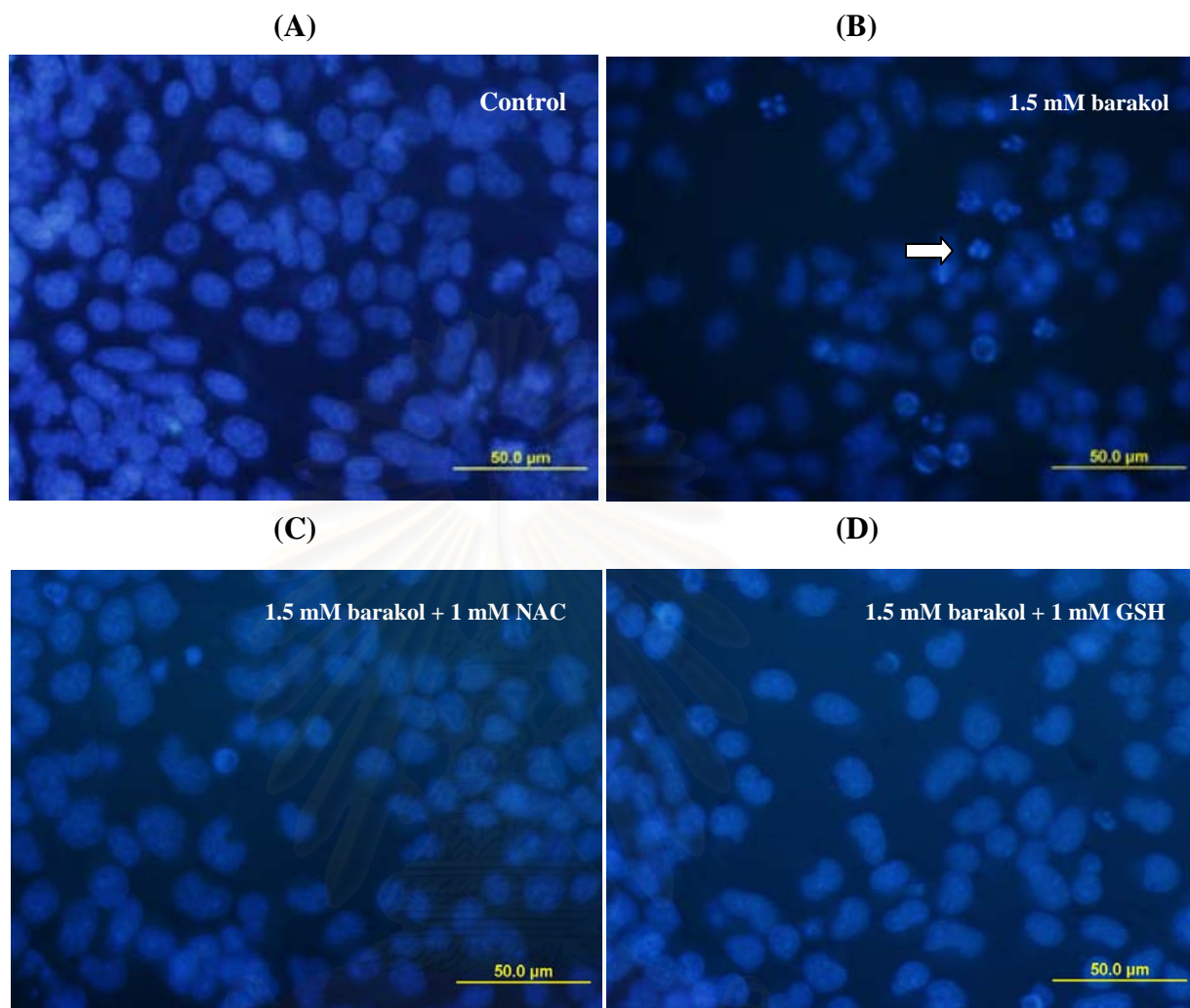


Figure 10 Hoechst 33342 staining analysis for the effects of antioxidants on barakol-treated P19 cells. (A) Viable cells as a control, showed bright round nuclei with Hoechst 33342 staining. (B) P19 cells were exposed to barakol (1.5 mM) for 24 h which displayed chromatin condensation (arrow). (C) P19 cells were pretreated with 1 mM NAC for 30 min before the addition of 1.5 mM barakol. After incubation for 24 h, viable cells showed bright round nuclei with Hoechst 33342 staining similar to control cells. (D) Cells were pretreated with 1 mM GSH for 30 min before the addition of 1.5 mM barakol. Scale bar = 50 μ m.

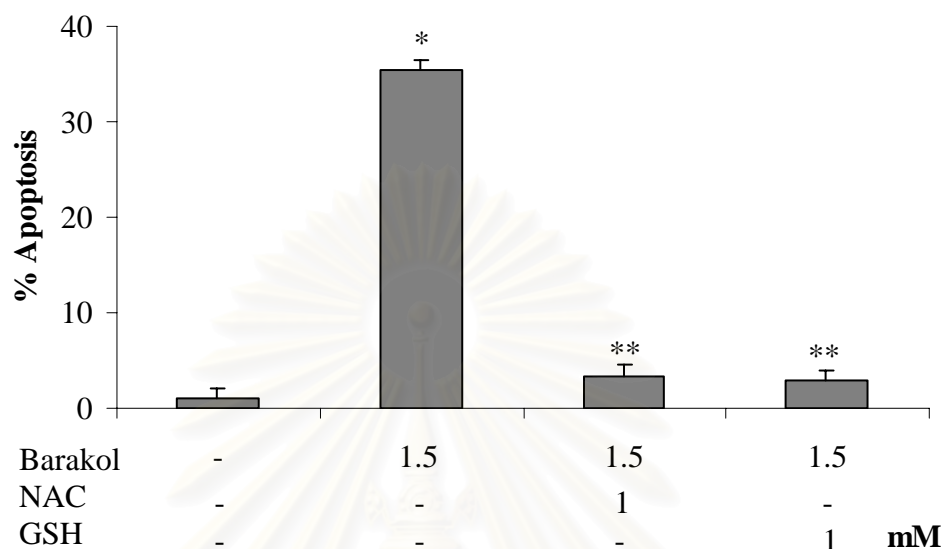


Figure 11 Effect of antioxidants, NAC and GSH, on barakol-induced apoptosis in P19 cells. Cells were pretreated with 1 mM NAC or 1 mM GSH and then treated with 1.5 mM barakol for 24 h. Apoptotic cells were determined by Hoechst 33342 analysis. The percentage of apoptotic cells in the presence of antioxidant and barakol or barakol alone was shown as bars. Each point represented the mean \pm SEM of three different experiments, each performed in triplicate. * $P < 0.05$ compared to the cells without barakol. ** $P < 0.05$ compared to the cells treated with barakol.

สถาบันวิทยบริการ
จุฬาลงกรณ์มหาวิทยาลัย

5. Measurement of intracellular ROS

5.1. Measurement of intracellular ROS formation induced by barakol

The Hoechst 33342 assay indicated that the antioxidants were able to protect barakol-induced apoptosis in P19 cells, revealing the mechanism by which barakol induced apoptosis via ROS generation. The intracellular ROS level was determined by using DCFH-DA staining and analyzed by flow cytometry. As shown in Figure 12A, a comparison of P19 cells exposed to barakol with control cells, there was a sharp increase in DCF intensity, and the intensity shifted to the right (Figure 12A). The intensities were 14.21, 17.90, 38.19, 40.51, and 27.67 after 15, 30, 60, 120, and 180 min of incubation with barakol (0.4 mM), respectively. A kinetic analysis of ROS production revealed that ROS burst could be detected as fast as 15 min after exposure to barakol. The DCF intensity of barakol-treated cells gradually increased and reached its maximum level at 120 min (Figure 12B). However, the DCF intensity of barakol-treated cells started to decrease at 180 min. The result indicated that barakol induced apoptosis in P19 cells through the generation of ROS.

5.2. Effect of antioxidants on the generation of ROS in barakol-treated P19 cells

To test whether the antioxidants effectively inhibited barakol-induced ROS generation, the intracellular ROS generation in response to the antioxidants was determined by using DCFH-DA dye and analyzed by flow cytometric analysis. The cells treated with barakol showed the 4.21 ± 0.46 fold increasing of DCF intensity when compared to the non-treated control. Cells treated with 0.5 μ M hydrogen peroxide for 30 minutes were used as a positive control (Ray et al., 2006). Pretreated with NAC or GSH showed the DCF intensity was almost reduced to the control level as shown in Figure 13A. The antioxidant NAC completely inhibited barakol-induced ROS generation as demonstrated by decreased DCF intensity to 1.45 ± 0.19 fold as well as GSH which decreased DCF intensity to 1.34 ± 0.2 fold as shown in Figure 13B (Table 9). As expected, both NAC and GSH can effectively inhibit barakol-induced ROS generation in P19 cells.

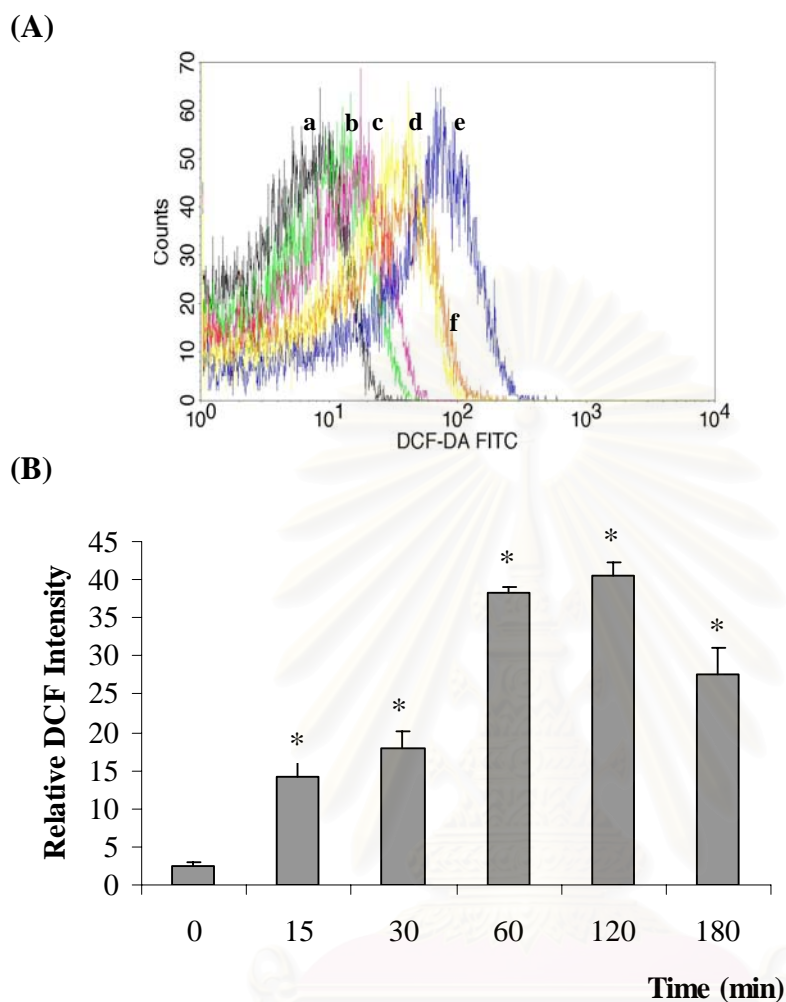


Figure 12 Time-dependent ROS formation in barakol-treated P19 cells. (A) Relative fluorescence intensity in P19 cells was quantitated by a flow cytometry using DCFH-DA staining. Cells were incubated with barakol free medium (a) or 0.4 mM barakol for 15 min (b), 30 min (c), 60 min (d), 120 min (e), 180 min (f). (B) The intensity of DCF in the presence of barakol treated cells was shown as bars. Each point represented mean \pm SEM of three independent experiments. * $P < 0.05$, significantly differed from the control group.

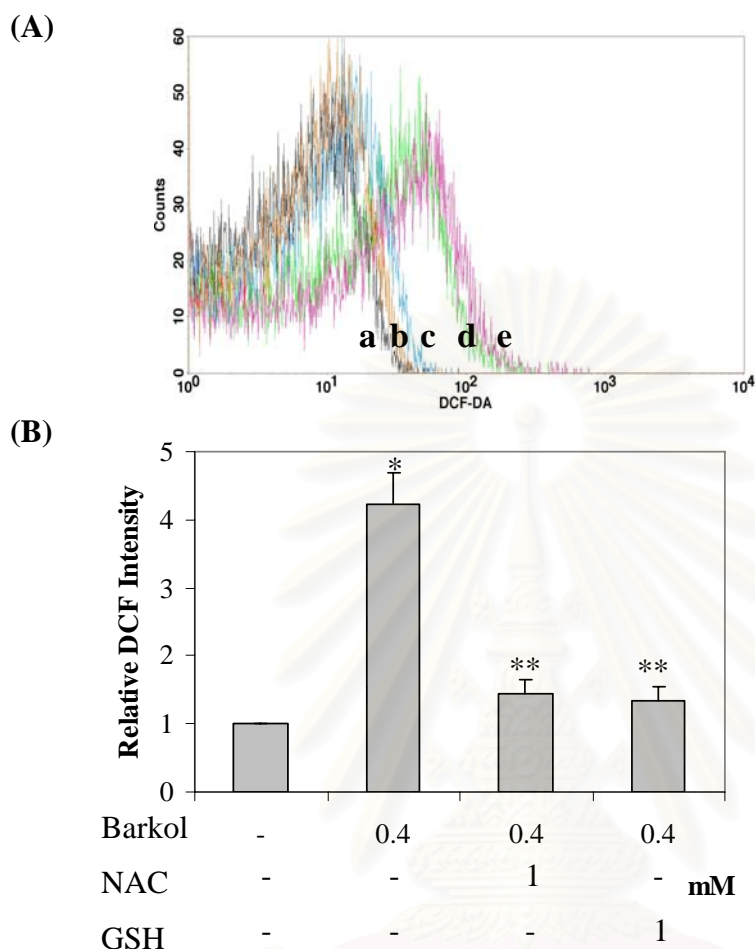


Figure 13 The effects of NAC and GSH on the generation of ROS induced by barakol using specific fluorescence dye DCFH-DA and analyzed by flow cytometry. (A) P19 cells were pretreated with NAC or GSH for 30 min, prior to the addition of 0.4 mM barakol and incubated for 2 h. The decreasing of fluorescence intensity in histogram showed (a) control, (b) with 1 mM GSH, (c) with 1 mM NAC, (d) 0.4 mM barakol (e) 0.5 μ M H_2O_2 (positive control). (B) The intensity in the presence of antioxidant with barakol or barakol alone was shown as bars. Each point represented mean \pm SEM of three independent experiments. * $P < 0.05$, significantly differed from the control group (no treatment). ** $P < 0.05$, significantly differed from 0.4 mM barakol-treated group.

5.3. Characterization of ROS

In biological tissues, $O_2^{\bullet-}$ can also be converted into the nonradical species H_2O_2 . In the presence of reduced transition metals (e.g., ferrous or cuprous ions), hydrogen peroxide can be converted into the highly reactive OH^{\bullet} (Evens et al., 2004). To identify the ROS involved in barakol-induced the generation of ROS, we measured ROS level in the presence of MnTBAP (a SOD mimetic) (Sawyer et al., 2005), catalase (a hydrogen peroxide scavenger) (Chen et al., 2003) and sodium formate (a hydroxyl radical scavenger) (Kuta et al., 2003). Treatment with 0.4 mM barakol resulted in a significant increase in the population of ROS levels, measured by monitoring the fluorescence intensity of DCFH-DA oxidized into the cells. Pretreatment of cells with 0.1 mM MnTBAP either in the presence or absence of barakol significantly increased in the superoxide level 3.67 ± 1.04 folds higher than cells exposed to barakol alone (2.16 ± 0.28 folds), suggesting that barakol did not affect superoxide anion level (Figure 14). The result suggested that barakol could not burst $O_2^{\bullet-}$ in the cells. Pretreatment with 30,000 unit/ml catalase had no significant change in ROS level comparing to the barakol-treated cells, indicating the absence of the involvement of hydrogen peroxide in this system (Figure 15). Since catalase could not convert H_2O_2 to water and oxygen, H_2O_2 might therefore be converted to OH^{\bullet} by Fenton reaction (Evens et al., 2004). Thus, OH^{\bullet} was measured using sodium formate, a hydroxyl radical scavenger. Pretreatment with 1 mM sodium formate completely abolished the effect of barakol-induced ROS generation while treatment with sodium formate alone did not show any difference from the control (Figure 16). Taken together with our previous results, the antioxidants NAC and GSH completely inhibited ROS generation, suggesting that the predominant ROS in barakol-induced apoptosis was hydroxyl radical.

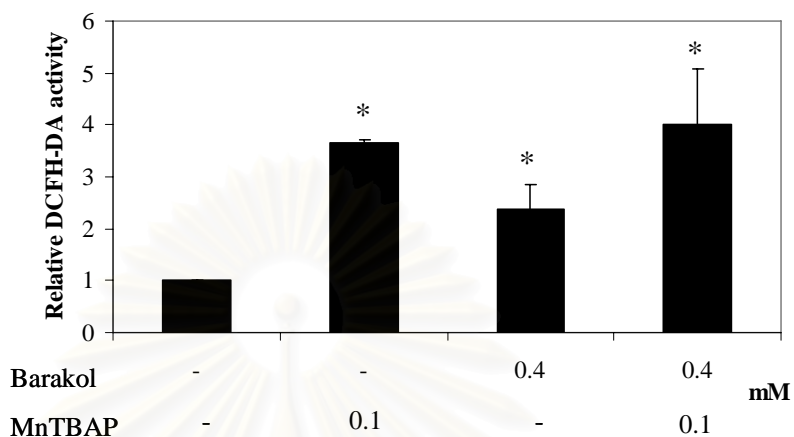


Figure 14 Effect of MnTBAP, a SOD mimetic, on barakol-treated cells analyzed by DCFH-DA staining. $O_2^{\bullet-}$ generation was defined by pretreatment with 0.1 mM MnTBAP for 30 min before treated with 0.4 mM barakol for 2 h. Each point represented mean \pm SEM of three independent experiments. * $P < 0.05$, significantly differed from the control group (no treatment).

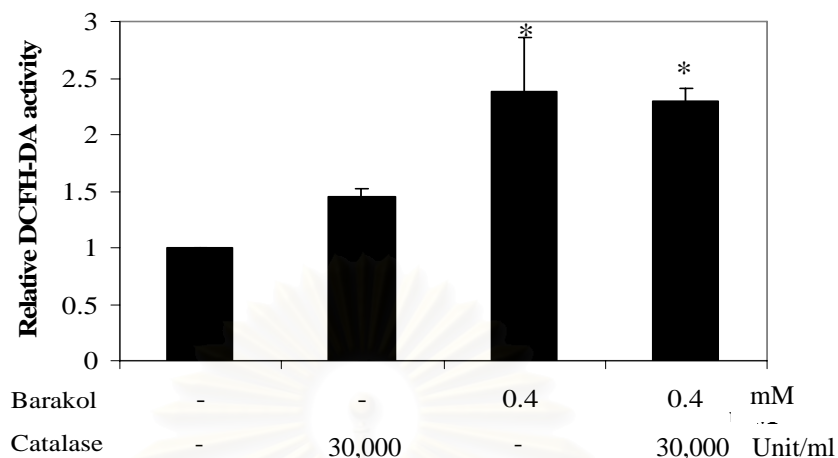


Figure 15 Effect of catalase, a hydrogen peroxide scavenger, on barakol-treated cells analyzed by DCFH-DA staining. H_2O_2 generation has elucidated by pretreatment with 30,000 unit/ml catalase for 30 min before treated with 0.4 mM barakol for 2 h. Each point represented mean \pm SEM of three independent experiments. * $P < 0.05$, significantly differed from the control group (no treatment).

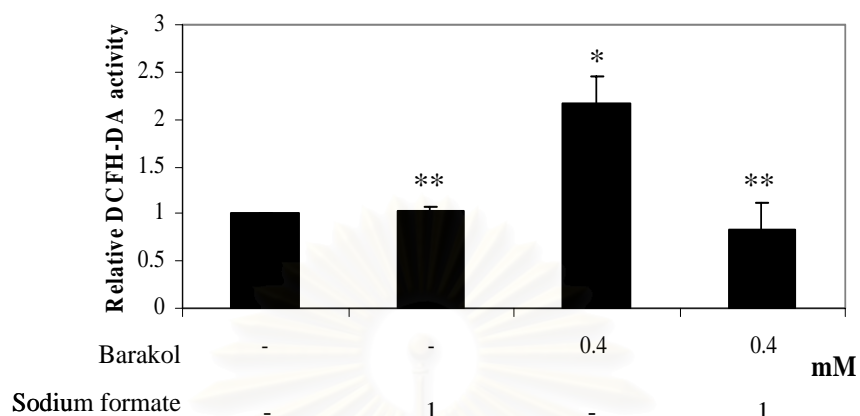


Figure 16 Effect of sodium formate, a hydroxyl radical scavenger, on barakol-treated cells analyzed by DCFH-DA staining. OH^\bullet generation has been elucidated by pretreatment with 1 mM sodium formate for 30 min before treated with 0.4 mM barakol for 2 h. Each point represented mean \pm SEM of three independent experiments. * $P < 0.05$, significantly differed from the control group (no treatment). ** $P < 0.05$ compared to the cells treated with barakol only.

6. Measurement of caspase-9 activity

Caspases are fundamental components of the mammalian apoptotic machinery. Caspase-9 is a prototypical caspase that becomes activated during apoptosis and can therefore be used as an apoptotic marker (Adams, 2003). For monitoring caspase-9 activity, P19 cells were treated with barakol at various concentrations for 24 h followed by the assay of caspase-9 activity. The activity of caspase-9 was analyzed by measuring the levels of 7-amino-4-trifluoromethyl coumarin (AFC) cleaved from the substrate LEHD-AFC. Parallel with the timing pattern of the appearance of the apoptotic cells, the caspase-9 activity increased in a dose-dependent manner (Figure 17). Caspase-9 activity significantly increased in response to 0.4 mM barakol (1.5 ± 0.02 folds). While barakol at the concentration of IC_{50} induced a gradual rise in caspase-9 activity a 2.13 ± 0.03 folds after 24 h exposure to barakol. These results indicated that signaling cascade leading to apoptosis in barakol-treated P19 cells involved in the generation of ROS followed by caspase-9 activation.

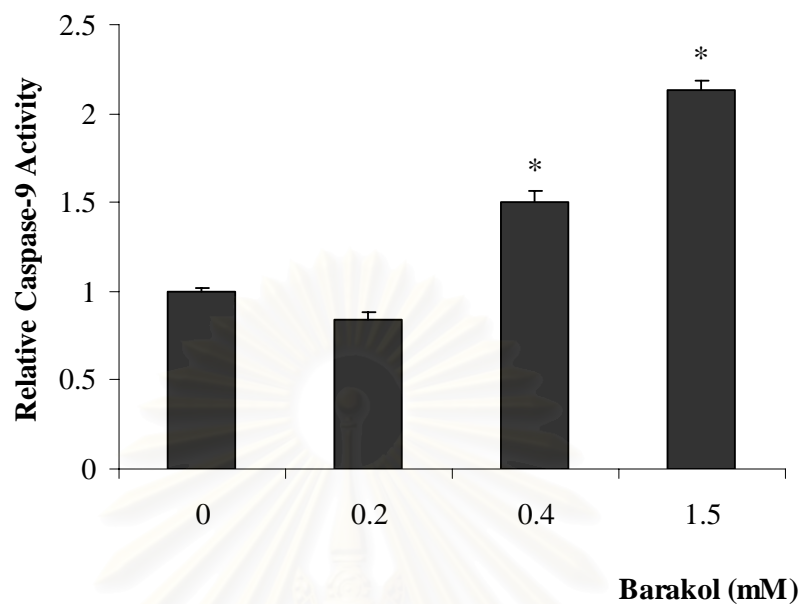


Figure 17 Measurement of caspase-9 activity. P19 cells were treated with barakol at concentrations ranging from 0.2 to 1.5 mM and incubated for 24 h followed by the assay of caspase-9 activity using a Fluorometric Assay Kit. Data were mean \pm SEM (n=3). * $P < 0.05$ as compared to non-treated control.

สถาบันวิทยบริการ
จุฬาลงกรณ์มหาวิทยาลัย

CHAPTER V

DISCUSSION AND CONCLUSION

Barakol is a biologically active constituent extracted from the leaves and flowers of *C. siamea*. This plant is widely cultivated in Southeast Asia including Thailand, and is traditionally used to treat insomnia, diabetes, fever, hypertension and constipation (Deachapunya et al., 2005). Barakol decreased spontaneous locomotor activity (Arunlakshana, 1949; Jantarayota, 1987) and displayed anxiolytic-like properties in the elevated plus-maze test in animal model (Thongsaard et al., 1996). In clinical studies, barakol has been shown the anxiolytic-like properties as well (Arunlakshana, 1949; Pooviboonsuk et al., 2000). Thus, barakol tablet in commercial brand are available for the treatment of insomnia. However, its toxicity was reported and became an important limitation of using this agent.

Barakol in alkaline solution is very rapidly degraded while in strong acids it forms anhydro-salt which is stable at room temperature (Bycroft et al., 1970). Barakol in water and incubated at 37 °C for 30 min were partly converted to other compounds as new peaks were observed (Thongsaard et al., 2001). In this study, the stability study of barakol in culture condition for the cytotoxicity testing was elucidated using HPLC technique. In the culture condition with cells, the percentage of barakol recovery slightly decreased ($12.7 \pm 1.9\%$) after 24 h which was nearly equal to in the condition without cells ($19.68 \pm 1.57\%$). In addition, a degraded product, exhibiting at a retention time 39.9 ± 1.6 min, could be observed after 24 h. The result implied that barakol was uptaken by P19 cells about 6.98% during 24-h incubation and the metabolism of treated cells did not affect barakol stability. The UV spectrum of barakol showed the λ_{\max} at 249 nm while the λ_{\max} of the degraded product was 291 nm, where structure determination should be further elucidated. Since barakol was mostly stable in cell culture condition during 24-h incubation, we therefore performed mitochondrial dysfunction testing using XTT assay during this period.

Incubation of P19 cells with barakol caused cytotoxicity in a concentration-dependent manner by exhibiting an IC_{50} value at 1.5 mM. Treatment with barakol (1.5 mM) resulted in significant decrease in cell survival approximately $12.4 \pm 0.59\%$ within

the first 12 h and gradually decreased until 24 h. The result showed that barakol could cause the mitochondrial dysfunction analyzed by XTT assay (Kuo et al., 2006; Lu et al., 1997). These methods commonly monitor PMS mediated reduction of tetrazolium by various NAD (P) dependent dehydrogenases (Su et al., 2005). From the XTT assay, the mitochondria of P19 cells have lost their permeability first after treated with barakol.

To investigate the death pattern, staining with Hoechst 33342 was used to determine the early stage and late stage of apoptosis (Piiper et al., 2002). The significant decrement in vital cell number with accompanied by the chromatin condensation and nuclear cleavage, which are typical morphological features of apoptotic cells (Lin. et al, 2003). Barakol can induce P19 cells to apoptosis in a concentration-dependent manner analyzed by Hoechst 33342 staining, suggesting that barakol-treated P19 cells for 24 h indicated an early apoptosis (Figure 8). The staining with PI, a well known dye for the detection of late apoptotic (Lecoeur, 2002), was used to clarify DNA content of P19 cells which exposed to barakol. DNA content of treated cells was then determined by flow cytometric analysis. Barakol (1.5 mM) slightly induced an accumulation of cells in sub G₀/G₁ phase at 24 h but significantly decreased G₀/G₁ phase when compared to control cells, suggesting the cell cycle arrest in P19 cells (Schmidt-Kastner et al., 1998; Sehlmeier et al., 1996). We found that the percentage of apoptotic cells induced by barakol detected by Hoechst 33342 and PI staining was less than the percentage of cell viability detected by XTT assay. The result indicated that barakol disturbed the mitochondrial function leading to induced mainly early apoptosis after 24 h incubation. Therefore, the apoptotic mechanism was further investigated. Several studies have been reported that ROS caused mitochondrial dysfunction by disturbing the equilibrium of pro-apoptotic and anti-apoptotic proteins and loss of the mitochondrial transmembrane potential (Ouyang et al., 2004; Su et al., 2005; Lee et al., 2005).

From the previous study, barakol decreased GSH in HepG2 cells (Lawanprasert et al., 2001). This report led us to examine the correlation between barakol-induced apoptosis and ROS generation. To clarify ROS-dependent apoptotic mechanism, Hoechst 33342 staining showed that pretreatment with NAC or GSH significantly decreased apoptotic cells. The result indicated that ROS played an important role in barakol-induced apoptosis. Mitochondria play a central role in cell death by controlling

cellular energy metabolism, production of ROS, resulting in the release apoptotic factors into the cytosol when its mitochondrial permeability is dysfunction. DCFH-DA dye has been widely used as a relatively nonspecific intracellular probe for ROS. The DCFH-DA dye is nonpolar and crosses cell membrane readily. Moreover, within the cell it is hydrolyzed by cytosolic esterase to DCFH, which rapidly reacts with ROS to form fluorescence DCF (McArdle et al., 2005). Thus, measurement of cytosolic ROS generated by barakol were further performed using DCFH-DA analyzed by flow cytometer. The fluorescence intensity of DCF in barakol-treated cells increased when compared to the control and peaking at 2 h. The generation of ROS might cause mitochondrial dysfunction (Ouyang et al., 2004; Lee et al., 2005). Pretreatment of P19 cells with GSH or NAC prior to barakol exposure analyzed by DCFH-DA staining inhibited the ROS generation. The result demonstrated that barakol could affect the ROS level in P19 cells. Thus the type of ROS promoted by barakol would be elucidated.

In maintenance of redox homeostasis, enzyme SOD converts $O_2^{\bullet-}$ into H_2O_2 which is further converted into water by catalase or glutathione peroxidase (Droge, 2002). To define ROS, pretreatment with MnTBAP (a SOD mimetic), catalase (a H_2O_2 scavenger) or sodium formate (a OH^{\bullet} scavenger) was further used and analyzed by flow cytometer (Houstis et al., 2006). Pretreated with MnTBAP, ROS level in cells increased higher than in barakol-treated cells. The result showed that barakol did not affect the production of $O_2^{\bullet-}$. It is known that $O_2^{\bullet-}$ would be converted to H_2O_2 by the enzymatic reaction catalyzed by SOD. Under normal physiological conditions, H_2O_2 is converted into H_2O by catalase. Then, catalase was used to indicate that H_2O_2 might involve in the apoptotic mechanism of barakol-treated cells. However, pretreatment with catalase prior to barakol exposure had no significant change in ROS signal when comparing to the cells treated with barakol alone. The result indicated that H_2O_2 did not play a role in barakol-induced apoptosis, otherwise catalase could decrease the ROS signal after barakol treatment. In general, if there is imbalance between H_2O_2 and enzymatic reaction catalyzed by catalase, H_2O_2 could react with Fe^{2+} in order to convert to OH^{\bullet} via a Fenton reaction (Cadenas and Davies, 2000). Since catalase could not eradicate cellular ROS level, indicating that H_2O_2 could not absolutely convert to H_2O . To define the role OH^{\bullet} , pretreated with sodium formate prior to barakol exposure was implemented. The result

showed the decline of ROS level, indicating that OH^\bullet played an important role in the generation of ROS in barakol-treated cells.

Several studies were reported that ROS could play a critical role in mediating caspase dependent of cell death by promoting cytochrome *c* release. Clearly, it seems to be multiple levels of fail-safe mechanisms in regulating cytochrome *c*-mediated activation of caspases (Chen et al., 2003). Two principal pathways to caspase activation have been recognized. One is triggered by engagement of so called “death receptors” on the cell surface (Strasser et al., 2000; Ashkenazi et al., 1999). The other, of more ancient origin, is provoked by various forms of stress, including inadequate cytokine support and diverse types of intracellular damage. The stress pathway instead typically activates caspase-9 via the scaffold protein Apaf-1. A conformational change in Apaf-1, induced by cytochrome *c* from damaged mitochondria, allows it to recruit procaspase-9 via their homologous caspase recruitment domains (CARDs) and to oligomerize into a heptameric scaffold (Acehan et al. 2002). In the resulting giant (~1 megadalton) “apoptosome”, caspase-9 is activated primarily by allosteric change and dimerization rather than cleavage (Rodriguez and Lazebnik 1999; Boatright et al., 2003). The apoptosome then processes caspase-3 and caspase-7, which initiate robust proteolysis and free a dedicated DNase (CAD/DFF40) that dices the chromatin (Enari et al., 1998). Thus the caspase-9 activity was then performed to clarify the cellular downstream apoptosis, the mitochondria-dependent pathway in barakol-treated cells. The caspase-9 activity increased in barakol-treated P19 cells after 24 h incubation in a concentration-dependent manner. The results demonstrated that barakol-induced apoptosis involved the activation of caspase-9. Taken together, apoptosis induced by barakol was mediated through the generation of ROS and the activation of caspase-9 activity.

In conclusion, the present study showed that barakol-mediated ROS generation represented the central trigger for activation of the apoptotic signaling cascade. Exposure of P19 cells to barakol resulted in the accumulation of ROS leading to mitochondrial dysfunction. Then OH^\bullet diffused from the mitochondria into cytosol, resulted in the activation of caspase-9, which then processes and activates other downstream caspases, such as caspase-3, to exhibit the biochemical execution of apoptosis in P19 cells (Figure 18). Our studies reveal that barakol induces apoptosis in P19 cells, which are pluripotent

embryonic stem cells. Thus, barakol should be considered not to be taken during pregnancy because it might cause birth defects. Moreover, antioxidants could be recommended for the treatment of patients affected by an overdose of barakol.



สถาบันวิทยบริการ
จุฬาลงกรณ์มหาวิทยาลัย

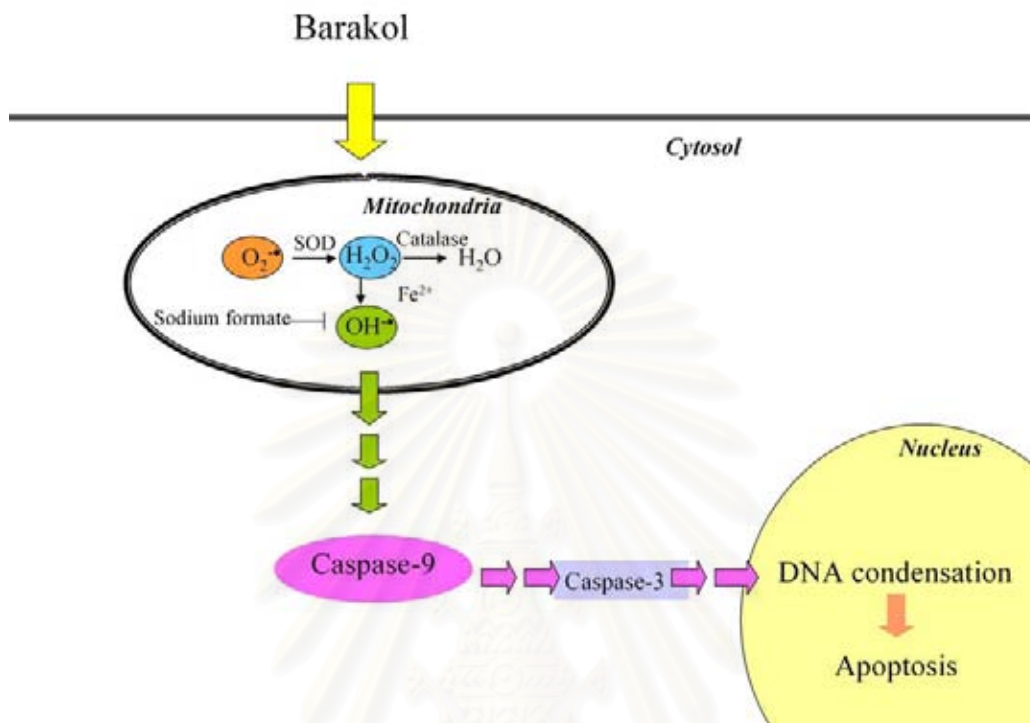


Figure 18 Schematic illustrating signaling cascade affected by barakol in P19 cells.

สถาบันวิทยบริการ
จุฬาลงกรณ์มหาวิทยาลัย

REFERENCES

- Acehan, D., Jiang, X., Morgan, D.G., Heuser, J.E., Wang, X., Akey, C.W. 2002. Three-dimensional structure of the apoptosome: implications for assembly, procaspase-9 binding, and activation. Mol. Cell 9(2): 423-432.
- Adams, J.M. 2003. Ways of dying: multiple pathways to apoptosis. Genes Dev.17: 2481-2495.
- Arunlakshana, O., 1949. Studies of indigenous drugs: 1. Pharmacological actions of leaves of *Cassia siamea*. Siriraj Hospital Gaz. 1: 434-443.
- Ashkenazi, A., Dixit, V.M. 1999. Apoptosis control by death and decoy receptors. Curr. Opin. Cell. Biol. 11: 255-260.
- Bain, G., Gottlieb, D.I. 1994. Expression of retinoid X receptors in P19 embryonal carcinoma cells and embryonic stem cells. Biochem. Biophys. Res. Commun. 200(3): 1252-1256.
- Bandyopadhyay, U., Das Dipak Banerjee, K.R. 1999. Reactive oxygen species: Oxidative damage and pathogenesis. Current Science 77(5): 658-666.
- Bello, R.I., Gomez-Diaz, C., Lopez-Lluch, G., Forthoffer, N., Cordoba-Pedregosa, M.C., Navas, P., Villalba, J.M. 2005. Dicoumarol relieves serum withdrawal-induced G0/1 blockade in HL-60 cells through a superoxide-dependent mechanism. Biochem. Pharmacol. 69(11): 1613-1625.
- Boatright, K.M., Salvesen, G.S. 2003. Mechanisms of caspase activation. Curr. Opin. Cell Biol. 15(6): 725-731.
- Boldyrev, A.A., 2000. Discrimination between apoptosis and necrosis of neurons under oxidative stress. Biochemistry (Mosc.) 658: 34-42.
- Bycroft, B.W., Hassanali-Walji, A., Johnson, A., King, T.J. 1970. The structure and synthesis of barakol: A novel dioaxaphenalene derivative from *Cassia siamea*. J. Chem. Soc. 12: 1686-1689.
- Cadenas, E., Davies, K.J. 2000. Mitochondrial free radical generation, oxidative stress, and aging. Free Radical Biol. Med. 29(3-4): 222-230.

- Chaichantipyuth, C., 1979. A photochemical study of the leaves of *Cassia siamea* Lam. and *Cassia spectabilis* D.C. M.Sc. thesis, Faculty of Pharmaceutical Sciences, Chulalongkorn University, Bangkok.
- Chen, Q., Crosby, M., Almasan, A. 2003. Redox regulation of apoptosis before and after cytochrome *c* Release. *Korean J. Biol. Sci.* 7(1): 1-9.
- Cheng, A.C., Huang, T.C., Lai, C.S., Pan, M.H. 2005. Induction of apoptosis by luteolin through cleavage of Bcl-2 family in human leukemia HL-60 cells. *Eur. J. Pharmacol.* 509(1): 1-10.
- Chiou, T.J., Tzeng, W.F. 2000. The roles of glutathione and antioxidant enzymes in menadione-induced oxidative stress. *Toxicology* 154(1-3): 75-84.
- Coyle, I., Wayner, M.J., Singer, G. 1976. Behavioral teratogenesis: a critical evaluation. *Pharmacol. Biochem. Behav.* 4(2):191-200.
- Deachapunya, C., Thongsaard, W., Poonyachoti, S. 2005. Barakol suppresses norepinephrine-induced inhibition of spontaneous longitudinal smooth muscle contractions in isolated rat small intestine. *J. Ethnopharmacol.* 101(1-3): 227-232.
- Droge, W. 2002. Free radicals in the physiological control of cell function. *Physiol. Rev.* 82(1):47-95.
- Enari, M., Sakahira, H., Yokoyama, H., Okawa, K., Iwamatsu, A., Nagata, S. 1998. A caspase-activated DNase that degrades DNA during apoptosis, and its inhibitor ICAD. *Nature* 391(6662): 43-50.
- Evens, A.M., Mehta, J., Gordon, L.I. 2004. Rust and corrosion in hematopoietic stem cell transplantation: the problem of iron and oxidative stress. *Bone Marrow Transpl.* 34(7): 561-571.
- Friesen, C., Herr, I., Krammer, P.H., and Debatin, K.M. 1996. Involvement of the CD95 (APO-1/Fas) receptor/ligand system in drug-induced apoptosis in leukemia cells. *Nat. Med.* 2: 574-577.
- Glozak, M.A., Rogers, M.B. 1996. Specific induction of apoptosis in P19 embryonal carcinoma cells by retinoic acid and BMP2 or BMP4. *Dev. Biol.* 179(2): 458-470.
- Green, D. R., Reed, J. C. 1998. Mitochondria and apoptosis. *Science* 281: 1309-1312.
- Hassanali-Walji, A., King, T.J., Wallwork, S.C., 1969. Barakol, a novel dioxaphenalene derivative from *Cassia siamea*. *J. Chem. Soc. Chem. Commun.* 12: 678.

- Hongsirinirachorn, M., Threeprasertsuk, S., Chutaputti, A. 2003. Acute hepatitis associated with barakol. J. Med. Assoc. Thai. 86: S484-489.
- Houstis, N., Rosen, E.D., Lander, E.S. 2006. Reactive oxygen species have a causal role in multiple forms of insulin resistance. Nature 440(7086): 944-948.
- Hsieh, T.J., Liu, T.Z., Lu, F.J., Hsieh, P.Y., Chen, C.H. 2005. Actinodaphnine induces apoptosis through increased nitric oxide, reactive oxygen species and down-regulation of NF-kappaB signaling in human hepatoma Mahlavu cells. Food Chem. Toxicol. 44(3): 344-354.
- Jantarayota, P. 1987. Effects of barakol extracted from leaves of *Cassia siamea* on the central nervous system. Thesis submitted for the degree of Master of Science in Pharmacy, Chulalongkorn University, Bangkok.
- Jin, Z.G., Liu, L., Zhong, H., Zhang, K.J., Chen, Y.F., Bian, W., Cheng, L.P, Jing, N.H. 2006. Second intron of mouse nestin gene directs its expression in pluripotent embryonic carcinoma cells through POU factor binding site. Acta. Biochim. Biophys. Sin. (Shanghai) 38(3): 207-212.
- Jones-Villeneuve, E.M., Rudnicki, M.A., Harris, J.F., McBurney, M.W. 1983. Retinoic acid-induced neural differentiation of embryonal carcinoma cells. Mol. Cell. Biol. 3(12): 2271-2279.
- Jung, C.G., Kim, H.J., Kawaguchi, M., Khanna, K.K., Hida, H., Asai, K., Nishino, H., Miura, Y. 2005. Homeotic factor ATBF1 induces the cell cycle arrest associated with neuronal differentiation. Development 132(23): 5137-5145.
- Kadenbach, B., Arnold, S., Lee, I., Huttemann, M. 2004. The possible role of cytochrome *c* oxidase in stress-induced apoptosis and degenerative diseases. Biochim. Biophys. Acta. 1655(1-3): 400-408.
- Kamel, N.S, Gammack, J.K. 2006. Insomnia in the elderly: cause, approach, and treatment. Am. J. Med. 119(6): 463-469.
- Kiechle, F.L., Zhang, X. 2002. Apoptosis: biochemical aspects and clinical implications. Clin. Chim. Acta. 326(1-2): 27-45.
- Kling, D.E., Aidlen, J.T., Fisher, J.C., Kinane, T.B., Donahoe, P.K., Schnitzer, J.J. 2005. Nitrofen induces a redox-dependent apoptosis associated with increased p38 activity in P19 teratocarcinoma cells. Toxicol. In Vitro. 19(1): 1-10.

- Kluza, J., Mazinghien, R., Degardin, K., Lansiaux, A., Bailly, C. 2005. Induction of apoptosis by the plant alkaloid sampangine in human HL-60 leukemia cells is mediated by reactive oxygen species. Eur. J. Pharmacol. 525: 32–40.
- Kuo, Y.C., Kuo, P.L., Hsu, Y.L., Cho, C.Y., Lin, C.C. 2006. Ellipticine induces apoptosis through p53-dependent pathway in human hepatocellular carcinoma HepG2 cells. Life Sci. 78(22): 2550-2557.
- Kuta, D.D., Gaivaronskaya, L.M. 2003. Ca²⁺ and reactive oxygen species are involved in the defense responses of rice callus culture to rice blast disease. Afr. J. Biotechnol. 3 (1): 76-81.
- Lawanprasert, S., Chaichantipyuth, C., Unchern, S., Lawanprasert, Y., Clair, St. D. 2001. In vitro hepatotoxicity study of barakol using human hepatoma cell line HepG2. Thai J. Pharm. Sci. 25(3-4): 149-159.
- Lecoeur, H. 2002. Nuclear apoptosis detection by flow cytometry: influence of endogenous endonucleases. Exp. Cell. Res. 277(1): 1-14.
- Lee, C.S., Kim, Y.J., Ko, H.H., Han, E.S. 2005. Inhibition of 1-methyl-4-phenylpyridinium-induced mitochondrial dysfunction and cell death in PC12 cells by sulfonyleurea glibenclamide. Eur. J. Pharmacol. 527(1-3): 23-30.
- Lin, J.S., Park, M.K., Nahm, M.H. 2001. Chromogenic assay measuring opsonophagocytic killing capacities of antipneumococcal antisera. Clin. Diagn. Lab Immunol. 8(3): 528-533.
- Lin, S., Fujii, M., Hou, D.X. 2003. Rhein induces apoptosis in HL-60 cells via reactive oxygen species-independent mitochondrial death pathway. Arch. Biochem. Biophys. 418: 99–107.
- Liu, B., Hattori, N., Zhang, N.Y., Wu, B., Yang, L., Kitagawa, K., Xiong, Z.M., Irie, T., Inagaki, C. 2005. Anxiolytic agent, dihydrohonokiol-B, recovers amyloid beta protein-induced neurotoxicity in cultured rat hippocampal neurons. Neurosci. Lett. 384 (1-2): 44-47.
- Lu, J.H., Chiu, Y.T., Sung, H.W., Hwang, B., Chong, C.K., Chen, S.P., Mao, S.J., Yang, P.Z., Chang, Y. 1997. XTT-colorimetric assay as a marker of viability in cryoprocessed cardiac valve. J. Mol. Cell. Cardiol. 29(4): 1189-1194.

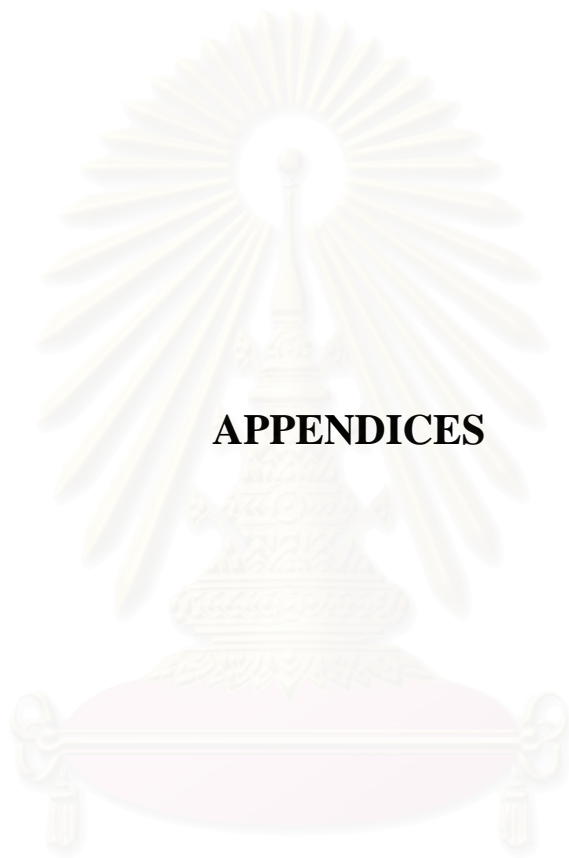
- McArdle, F., Pattwell, D.M., Vasilaki, A., McArdle, A., Jackson, M.J. 2005. Intracellular generation of reactive oxygen species by contracting skeletal muscle cells. Free Radical. Biol. Med. 39(5): 651-657.
- McBurney, M.W., Rogers, B.J. 1982. Isolation of male embryonal carcinoma cells and their chromosome replication patterns. Dev. Biol. 89(2):503-508.
- McBurney MW. 1993. P19 embryonal carcinoma cells. Int. J. Dev. Biol. 37(1): 135-140
- Muller, M., Strand, S., Hug, H., Heinemann, E.M., Walczak, H., Hofmann, W.J., Stremmel, W., Krammer, P.H., and Galle, P.R. 1997. Drug-induced apoptosis in hepatoma cells is mediated by the CD95 (APO-1/Fas) receptor/ligand system and involves activation of wild-type p53. J. Clin. Invest. 99: 403-413.
- Nagata, S. 1997. Apoptosis by death factor. Cell 88: 355-365.
- Nagele, R.G., Pietrolungo, J.F., Kosciuk, M.C., Lee, H., Roisen, F.J. 1983. Diazepam inhibits the spreading of chick embryo fibroblasts. Exp. Cell. Res. 143(1): 153-162.
- Nicoletti, I., Migliorati, G., Pagliacci, MC., Grignani, F., Riccardi, C. 1991. A rapid and simple method for measuring thymocyte apoptosis by propidium iodide staining and flow cytometry. J. Immunol. Methods. 139(2): 271-279.
- Nunes, M.L., Cavalcante, V. 2005. Clinical evaluation and treatment of insomnia in childhood. J. Pediatr. (Rio J). 81(4): 277-86.
- Ohshima, S. 2004. Apoptosis in stress-induced and spontaneously senescent human fibroblasts. Biochem. Biophys. Res. Commun. 324: 241-246.
- Ornoy, A., Arnon, J., Shechtman, S., Moerman, L., Lukashova, I. 1998. Is benzodiazepine use during pregnancy really teratogenic? Reprod. Toxicol. 12(5): 511-515.
- Ouyang, Y.B., Giffard, R.G. 2004. Changes in astrocyte mitochondrial function with stress: effects of Bcl-2 family proteins. Neurochem. Int. 45(2-3): 371-379.
- Pae, H.O., Oh, G.S., Choi, B.M., Seo, E.A., Oh, H., Shin, M.K., Kim, T.H., Kwon, T.O., Chung, H.T. 2003. Induction of apoptosis by 4-acetyl-12,13-epoxy-9-trichothecene-3,15-diol from *Isaria japonica* Yasuda through intracellular reactive oxygen species formation and caspase-3 activation in human leukemia HL-60 cells. Toxicol. in Vitro 17: 49-57.

- Pan, W., Jia, Y., Wang, J., Tao, D., Gan, X., Tsiokas, L., Jing, N., Wu, D., Li, L. 2005. Beta-catenin regulates myogenesis by relieving I-mfa-mediated suppression of myogenic regulatory factors in P19 cells. Proc. Natl. Acad. Sci. U.S.A. 102(48): 17378-17383.
- Paquin, J., Danalache, B.A., Jankowski, M., McCann, S.M., Gutkowska, J. 2000. Oxytocin induces differentiation of P19 embryonic stem cells to cardiomyocytes. Proc. Natl. Acad. Sci. U.S.A. 99(14): 9550-9555.
- Piiper, A., Dikic, I., Lutz, M.P., Leser, J., Kronenberger, B., Elez, R., Cramer, H., Muller-Esterl, W., Zeuzem, S. 2002. Cyclic AMP induces transactivation of the receptors for epidermal growth factor and nerve growth factor, thereby modulating activation of MAP kinase, Akt, and neurite outgrowth in PC12 cells. J. Biol. Chem. 277(46): 43623-43630.
- Pooviboonsuk, P., Tappayuthpijarn, P., Hinchearanund, T. 2000. Hypnotic effect of modified herbal extract from *cassia siamea*. in human subjects. J. Psychiatr. Assoc. Thailand 45: 251-259.
- Ray, S., Atkuri, K.R., Deb-Basu, D., Adler, A.S., Chang, H.Y., Herzenberg, L.A., Felsher, D.W. 2006. MYC can induce DNA breaks in vivo and in vitro independent of reactive oxygen species. Cancer Res. 66(13):6598-6605.
- Rehemtulla, A., Hamilton, C.A., Chinnaiyan, A.M., and Dixit, V.M. 1997. Ultraviolet radiation-induced apoptosis is mediated by activation of CD-95 (Fas/APO-1). J. Biol. Chem. 272: 25783-25786.
- Rodriguez, J., Lazebnik, Y. 1999. Caspase-9 and Apaf-1 form an active holoenzyme. Genes Dev. 13(24): 3179-3184.
- Saeki, K., Kobayashi, N., Inazawa, Y., Zhang, H., Nishitoh, H., Ichijo, H., Saeki, K., Isemura, M., You, A. 2002. Oxidation-triggered c-Jun N-terminal kinase (JNK) and p38 mitogen-activated protein (MAP) kinase pathways for apoptosis in human leukaemic cells stimulated by epigallocatechin-3-gallate (EGCG): a distinct pathway from those of chemically induced and receptor-mediated apoptosis. Biochem. J. 368(Pt 3): 705-720.
- Sahota, P.K., Jain, S.S., Dhand, R. 2003. Sleep disorders in pregnancy. Curr. Opin. Pulm. Med. 9(6): 477-83.

- Salzman, C. 1991. The APA task force report on benzodiazepine dependence, toxicity and abuse. Am. J. Psychiat. 148: 151-152.
- Sawyer, R.T., Dobis, D.R., Goldstein, M., Velsor, L., Maier, L.A., Fontenot, A.P., Silveira, L., Newman, L.S., Day, B.J. 2005. Beryllium-stimulated reactive oxygen species and macrophage apoptosis. Free. Radic. Biol. Med. 38(7):928-937.
- Schild, L., Bukowska, A., Gardemann, A., Polczyk, P., Keilhoff, G., Tager, M., Dudley, S.C., Klein, H.U., Goette, A., Lendeckel, U. 2006. Rapid pacing of embryoid bodies impairs mitochondrial ATP synthesis by a calcium-dependent mechanism-A model of in vitro differentiated cardiomyocytes to study molecular effects of tachycardia. Biochim. Biophys. Acta. 1762(6): 608-615.
- Schmidt-Kastner, P.K., Jardine, K., Cormier, M., McBurney, M.W. 1998. Absence of p53-dependent cell cycle regulation in pluripotent mouse cell lines. Oncogene 16: 3003-3011.
- Schweyer, S., Soruri, A., Heintze, A., Radzun, HJ., Fayyazi, A. 2004. The role of reactive oxygen species in cisplatin-induced apoptosis in human malignant testicular germ cell lines. Int. J. Oncol. 25(6): 1671-1676.
- Scott, M.D. 2006. H₂O₂ injury in beta thalassemic erythrocytes: Protective role of catalase and the prooxidant effects of GSH. Free Radical. Biol. Med. 40(7): 1264-1272.
- Sehlmeyer, U., Meister, A., Beisker, W., Wobus, A.M. 1996. Low mutagenic effects of mitomycin C in undifferentiated embryonic P19 cells are correlated with efficient cell cycle control. Mutat. Res. 354(1): 103-112.
- Shao, R., Karunagaran, D., Zhou, B.P., Li, K., Lo, S.S., Deng, J., Chiao, P., Hung, M.C. 1997. Inhibition of nuclear factor-kappaB activity is involved in E1A-mediated sensitization of radiation-induced apoptosis. J. Biol. Chem. 272(52): 32739-32742
- Strasser, A., Puthalakath, H., Bouillet, P., Huang, D.C., O'Connor, L., O'Reilly, L.A., Cullen, L., Cory, S., Adams, J.M. 2002. The role of bim, a proapoptotic BH3-only member of the Bcl-2 family in cell-death control. Ann. N.Y. Acad. Sci. 917: 541-548.

- Su, Y.T., Chang, H.L., Shyue, S.K., Hsu, S.L. 2005. Emodin induces apoptosis in human lung adenocarcinoma cells through a reactive oxygen species-dependent mitochondrial signaling pathway. Biochem. Pharmacol. 70(2): 229-241.
- Suwan, G., Sudsuang, R., Ghumma-Upakorn, D., Werawong, C. 1992. Hypertensive effects of barakol extracted from leaves of *Cassia siamea* Lam. in rats and cats. Thai. J. Physiol. Sci. 5: 53-65.
- Takahashi, A., Masuda, A., Sun, M., Centonze, V.E., Herman, B. 2003. Oxidative stress-induced apoptosis is associated with alterations in mitochondrial caspase activity and Bcl-2-dependent alterations in mitochondrial pH (pH_m). Brain. Res. Bull. 62(6): 497-504.
- Thongsaard, W., Deachapunya, C. Pongsakorn, S., Boyd, E. A., Bennett, G.W., Marsden, C.A. 1996. Barakol: A potential anxiolytic extracted from *Cassia siamea*. Pharmacol. Biochem. Behav. 53: 753-758.
- Thongsaard, W., Pongsakorn, S., Sudsuang, R., Bennett, G.W., Kendall, D.A., Marsden, C.A., 1997. Barakol, a natural anxiolytic, inhibits striatal dopamine release but not uptake in vitro. Eur. J. Pharmacol. 319: 157-164.
- Thongsaard, W., Chainakul, S., Bennett, G.W., Marsden, C.A., 2001. Determination of barakol extracted from *Cassia siamea* by HPLC with electrochemical detection. J. Pharm. Biomed. Anal. 25: 853-859.
- Tsukane, M., Yamauchi, T. 2006. Increase in apoptosis with neural differentiation and shortening of the lifespan of P19 cells overexpressing tau. Neurochem. Int. 48(4): 243-254.
- Wagner, H., El-Sayyad, S.M., Seligmann, O., Chari, V.M. 1978. Chemical constituents of *Cassia siamea* Lam, 2-methyl-5-acetonyl-7-hydroxychromone (cassiachromone). Planta. Med. 33: 258-261.
- Wang, J.Y.J. 2001. DNA damage and apoptosis. Cell Death Differ. 8: 1047-1048.
- Warrington, R.C., Norum, J.N., Hilchey, J.L., Watt, C., Fang, W.D. 2003. A simple, informative, and quantitative flow cytometric method for assessing apoptosis in cultured cells. Prog. Neuropsychopharmacol. Biol. Psychiatry. 27(2): 231-243.

- Westendorp, M.O., Frank, R., Ochsenbauer, C., Stricker, K., Dhein, J., Walczak, H., Debatin, K.M., and Krammer, P.H. 1995. Sensitization of T cells to CD95-mediated apoptosis by HIV-1 Tat and gp120. Nature 375: 497-500.
- Woodgate, A., MacGibbon, G., Walton, M., Dragunow, M. 1999. The toxicity of 6-hydroxydopamine on PC12 and P19 cells. Mol. Brain. Res. 69(1): 84-92.
- Wu, L.F., Li, G.P., Feng, J.L., Pu, Z.J. 2006. Molecular mechanisms adenosine-induced apoptosis in human HepG2 cells. Acta. Pharmacol. Sin. 27(4): 477-484.
- Xilouri, M., Papazafiri, P. 2006. Anti-apoptotic effects of allopregnanolone on P19 neurons. Eur. J. Neurosci. 23(1):43-54.
- Zhang, Z., Huang, C., Li, J., Leonard, S.S., Lanciotti, R., Butterworth, L., Shi, X. 2001. Vanadate-induced cell growth regulation and the role of reactive oxygen species. Arch Biochem Biophys. 392(2):311-320.



APPENDICES

สถาบันวิทยบริการ
จุฬาลงกรณ์มหาวิทยาลัย

APPENDIX A

PREPARATION OF REAGENTS

Growth medium of P19 cells

Alpha MEM powder (1 package) was dissolved with deionized water and the 2.3 g sodium bicarbonate was added. The medium was mixed well and adjusted pH to 7.2 with 5 N HCl. The medium was then adjusted volume to 1,000 ml and further sterilized by filtration with 0.2 μm milipore filter membrane. Before use, the medium was supplemented with 2.5% FBS and 7.5% NCS.

Phosphate buffered saline (PBS)

To make 1 liter of PBS, the ingredients including 8 g NaCl, 0.2 g KCl, 0.2 g KH_2PO_4 and 1.44 g Na_2HPO_4 were dissolved in deionized water. The solution was mixed well and adjusted the pH to 7.4 with 5 N NaOH. The solution was adjusted volume to 1,000 ml.

XTT solution

XTT powder 1 mg/ml was solubilized well in warm alpha MEM. The 25 μM PMS was added into XTT solution and mix well before used.

PMS stock solution

To prepare a stock solution 10 mM, PMS powder 3.063 mg/ml was solubilized well in PBS (use within 1 month).

PI stock solution

To prepare a stock solution 5 mg/ml, PI powder 5 mg was solubilized well in PBS 1 ml.

DCFH-DA stock solution

To prepare a stock solution 5 mM, DCFH-DA powder 2.29 mg was solubilized well in DMSO 1 ml.

Caspase-9 Fluorometric Assay Kit components

Cell Lysis Buffer	25	ml
2X Reaction Buffer	2	ml
LEHD-AFC (1 mM)	125	µl
DTT (1M)	100	µl

Assay Procedure (BioVision Research Products)

1. Induce apoptosis in cells by desired method. Concurrently incubate a control culture without induction.
2. Count cells and pellet $1-5 \times 10^6$ cells or use 50-200 µg cell lysates if protein concentration has been measured.
3. Resuspend cells in 50 µl of chilled Cell Lysis Buffer. Incubate cells on ice for 10 minutes.
4. Add 50 µl of 2x Reaction Buffer (containing 10 mM DTT) to each sample. Add 5 µl of the 1 mM LEHD-AFC substrate (50 µM final concentration) and incubate at 37 °C for 1-2 hour.
5. Read samples in a fluorometer equipped with a 400-nm excitation filter and 505-nm emission filter. For a plate-reading set-up, transfer the samples to a 96-well plate. Fold-increase in Caspase-9 activity can be determined by comparing these results with the level of the uninduced control.

APPENDIX B

TABLES OF EXPERIMENTAL RESULTS

Table 1 The peak area of barakol for standard curve analyzed by HPLC showing concentrations ranging from 0.0625 – 2 mM.

Barakol concentration (mM)	Peak area
0.0625	887752 ± 2338.7
0.125	1664842.6 ± 6219.1
0.25	3370432.3 ± 19165.9
0.5	6619480.34 ± 36738.3
1	13345472.3 ± 13339.7
2	27046884.6 ± 14295.6

Each value represented the mean value with SEM of three independent experiments.

Table 2 The percentage of recovery of barakol in culture condition at various time points analyzed by HPLC.

Time (h)	% Recovery of barakol with cells	% Recovery of barakol without cells
0 (control)	100 ± 0.00	100 ± 0.00
6	101.34 ± 4.66	96.56±1.69
18	95.04 ± 4.73	88.44±0.16
24	87.29 ± 1.96*	80.32±1.57

Each value represented the mean value with SEM of three independent experiments. Asterisks refer significant differences from the control group: * $P < 0.05$ determined by one-way ANOVA.

Table 3 The percentage of cytotoxicity of barakol-treated P19 cells in a concentration-dependent manner for 24 h.

Barakol (mM)	% Cell survival (compared to control)
0	100 ± 0.00
0.05	92.07 ± 0.17
0.1	92.11 ± 0.66
0.2	79.15 ± 3.15*
0.4	69.47 ± 4.92*
0.8	58.16 ± 6.62*
1	55.69 ± 5.64*
1.5	47.01 ± 2.53*
2	35.39 ± 10.49*
4	31.51 ± 7.49*

Each value represented the mean value with SEM of three independent experiments. Asterisks refer significant differences from the control group: * $P < 0.05$ determined by one-way ANOVA.

สถาบันวิทยบริการ
จุฬาลงกรณ์มหาวิทยาลัย

Table 4 The percentage of cytotoxicity of barakol-treated P19 cells at the IC₅₀ value (1.5 mM) at various time points (time dependency).

Time (hour)	%Cell survival (compared to control)
0	100 ± 0.00
6	107.47 ± 6.98
12	87.60 ± 0.59*
14	65.96 ± 4.22*
16	55.53 ± 0.73*
18	58.84 ± 1.12*
24	49.19 ± 0.49*

Each value represented the mean value with SEM of three independent experiments. Asterisks refer significant differences from the control group: * $P < 0.05$ determined by one-way ANOVA.

Table 5 The percentage of apoptotic cells, detected by Hoechst 33342 assay induced by barakol in a concentration-dependent manner for 24 h.

Barakol (mM)	% Apoptosis (compare to control)
0	0.0 ± 0.0
0.2	4.0 ± 1.0*
0.4	10.0 ± 1.0*
1	20.0 ± 2.0*
1.5	35.0 ± 1.0*

Each value represented the mean value of %control with SEM of three independent experiments. Asterisks refer significant differences from the control group: * $P < 0.05$ determined by one-way ANOVA

Table 6 The percentage of sub G₀/G₁ and G₀/G₁ phase by flow cytometry using propidium iodide, induced by barakol in a concentration-dependent manner for 24 h.

Barakol (mM)	% sub G ₀ /G ₁ phase	% G ₀ /G ₁ phase
control	2.38 ± 1.51	39.91 ± 6.22
0.4	4.08 ± 1.20	31.5 ± 1.36
1.5	6.01 ± 3.18	21.36 ± 2.33*

Each value represented the mean value of %control with SEM of three independent experiments for barakol-free medium (control) and barakol, and three independent experiments for the rest. Asterisks refer significant differences from the control group: * $P < 0.05$ determined by one-way ANOVA.

Table 7 The apoptotic percentage of barakol which pretreated P19 cells with 1 mM NAC or 1 mM GSH before the addition of barakol at its IC₅₀ (1.5 mM) for 24 h.

Treatment	% Apoptosis (compare to control)
-	1.0 ± 1.0
Barakol	35.34 ± 1.15*
Barakol + NAC	3 ± 1.0**
Barakol + GSH	3.34 ± 1.15**

Each value represented the mean value of %control with SEM of three independent experiments for control (barakol free) and barakol, and three independent experiments for the rest. * $P < 0.05$ compared to control, ** $P < 0.05$ compared to barakol only by one-way ANOVA.

Table 8 The fluorescence intensity in P19 cells quantitated by a flow cytometry using DCFH-DA, in response to 0.4 mM barakol treatment at various time points (time dependency).

Time (min)	Fluorescence Intensity
0	2.47 ± 0.45
15	14.21 ± 1.94*
30	17.90 ± 2.28*
60	38.19 ± 0.86*
120	40.51 ± 1.6*
180	27.67 ± 3.5*

Each value represented the mean value the relative fluorescence intensity of control with SEM of three independent experiments. Asterisks refer significant difference from the control group (time = 0): * $P < 0.05$ determined by One-way ANOVA.

Table 9 The DCFH-DA fluorescence intensity in P19 cells quantitated by a flow cytometry, in response to barakol treatment (0.4 mM), pretreatment with 1 mM NAC or 1 mM GSH prior to the addition of barakol and detected at 2 h after barakol treatment.

Treatment	Relative fluorescence intensity
-	1 ± 0.00
Barakol	4.21 ± 0.46*
Barakol + NAC	1.45 ± 0.19**
Barakol + GSH	1.34 ± 0.2**

Each value represented the mean value the relative fluorescence intensity of control with SEM of three independent experiments. Asterisks refer significant difference from the control group (no treatment): * $P < 0.05$ versus no treatment of barakol and ** $P < 0.05$ versus barakol treatment determined by One-way ANOVA.

Table 10 The fluorescence intensity in P19 cells quantitated by a flow cytometry using DCFH-DA, pretreatment with 0.1 mM MnTBAP before the addition of 0.4 mM barakol for 2 h.

Treatment	Relative fluorescence intensity
-	1 ± 0
MnTBAP	3.65 ± 0.05*
Barakol	2.16 ± 0.28*
Barakol+MnTBAP	3.67 ± 1.04*

Each value represented the mean value the relative fluorescence intensity of control with SEM of three independent experiments. Asterisks refer significant difference from the control group (no treatment): * $P < 0.05$ versus no treatment of barakol determined by One-way ANOVA.

Table 11 The fluorescence intensity in P19 cells quantitated by a flow cytometry using DCFH-DA, pretreatment with 30,000 unit/ml catalase before the addition of 0.4 mM barakol for 2 h.

Treatment	Relative fluorescence intensity
-	1 ± 0
Catalase	1.45 ± 0.05
Barakol	2.16 ± 0.28*
Barakol + catalase	1.93 ± 0.11*

Each value represented the mean value the relative fluorescence intensity of control with SEM of three independent experiments. Asterisks refer significant difference from the control group (no treatment): * $P < 0.05$ versus no treatment of barakol determined by One-way ANOVA.

Table 12 The fluorescence intensity in P19 cells quantitated by a flow cytometry using DCFH-DA, pretreatment with 1 mM sodium formate before the addition of 0.4 mM barakol for 2 h.

Treatment	Relative fluorescence intensity
-	1 ± 0
Sodium formate	1.03 ± 0.03**
Barakol	2.16 ± 0.28*
Barakol+Sodium formate	0.83 ± 0.28**

Each value represented the mean value the relative fluorescence intensity of control with SEM of three independent experiments. Asterisks refer significant difference from the control group (no treatment): * $P < 0.05$ versus no treatment of barakol and ** $P < 0.05$ versus barakol treatment determined by One-way ANOVA.

Table 13 Fluorometric assay of caspase-9 activity in P19 cells using caspase-9 fluorometric assay kit LEHD-AFC in response to barakol treatment.

Barakol (mM)	Relative caspase-9 activity
0	0.99 ± 0.02
0.2	0.83 ± 0.01
0.4	1.50 ± 0.02*
1.5	2.13 ± 0.03*
2	3.07 ± 0.05*

Each value represents the SEM. of three independent experiments. Asterisks refer significant difference from the control group (non-treated control): * $P < 0.05$ determined by One-way ANOVA.

Vita

Miss Supim Wongtongtair was born on March 16, 1978 in Lampang. She received her B.Sc. in Science (Medical Technology) from the Faculty of Allied Health Sciences, Chulalongkorn University in 2002.



สถาบันวิทยบริการ
จุฬาลงกรณ์มหาวิทยาลัย